FOSL1 promotes stem cell-like characteristics and anoikis resistance to facilitate tumorigenesis and metastasis in osteosarcoma by targeting SOX2

YANG WANG[1*], QIN HU[1,2*], YA CAO[3], LI YAO[1], HAORAN LIU[1,2], YAFENG WEN[4], YIXI BAO[5], SHUN ZHANG[1], CHUANZHU LV[1,6,7] and GUO-SHENG ZHAO[4]

[1]Department of Emergency Medicine Center, Sichuan Provincial People's Hospital, University of Electronic Science and Technology of China, Chengdu, Sichuan 610064, P.R. China; [2]Emergency and Trauma College, Hainan Medical University, Haikou, Hainan 571199, P.R. China; [3]Department of Pathology, Xinqiao Hospital, The Third Military Medical University, Chongqing 400037, P.R. China; [4]Department of Spine Surgery, The Second Affiliated Hospital of Chongqing Medical University, Chongqing 400010, P.R. China; [5]Department of Clinical Laboratory, The Second Affiliated Hospital of Chongqing Medical University, Chongqing 400010, P.R. China; [6]Research Unit of Island Emergency Medicine, Chinese Academy of Medical Sciences, Hainan Medical University, Haikou, Hainan 571199, P.R. China; [7]Key Laboratory of Emergency and Trauma of Ministry of Education, Hainan Medical University, Haikou, Hainan 571199, P.R. China

Received June 7, 2024; Accepted August 12, 2024

DOI: 10.3892/ijmm.2024.5418

Abstract. Metastasis is the leading cause of cancer-related death in osteosarcoma (OS). OS stem cells (OSCs) and anoikis resistance are considered to be essential for tumor metastasis formation. However, the underlying mechanisms involved in the maintenance of a stem-cell phenotype and anoikis resistance in OS are mostly unknown. Fos-like antigen 1 (FOSL1) is important in maintaining a stem-like phenotype in various cancers; however, its role in OSCs and anoikis resistance remains unclear. In the present study, the dynamic expression patterns of FOSL1 were investigated during the acquisition of cancer stem-like properties using RNA sequencing, PCR, western blotting and immunofluorescence. Flow cytometry, tumor-sphere formation, clone formation assays, anoikis assays, western blotting and *in vivo* xenograft and metastasis models were used to further investigate the responses of the stem-cell phenotype and anoikis resistance to FOSL1 overexpression or silencing in OS cell lines. The underlying molecular mechanisms were evaluated, focusing on whether SOX2 is crucially involved in FOSL1-mediated stemness and anoikis in OS. FOSL1 expression was observed to be upregulated in OSCs and promoted tumor-sphere formation, clone formation and tumorigenesis in OS cells. FOSL1 expression correlated positively with the expression of stemness-related factors (SOX2, NANOG, CD117 and Stro1). Moreover, FOSL1 facilitated OS cell anoikis resistance and promoted metastases by regulating the expression of apoptosis related proteins BCL2 and BAX. Mechanistically, FOSL1 upregulated SOX2 expression by interacting with the SOX2 promoter and activating its transcription. The results also showed that SOX2 is critical for FOSL1-mediated stem-like properties and anoikis resistance. The current findings indicated that FOSL1 is an important regulator that promotes a stem cell-like phenotype and anoikis resistance to facilitate tumorigenesis and metastasis in OS by regulating the transcription of SOX2. Thus, FOSL1 might represent an attractive target for therapeutic interventions in OS.

Correspondence to: Professor Chuanzhu Lv, Department of Emergency Medicine Center, Sichuan Provincial People's Hospital, University of Electronic Science and Technology of China, West Section 2, 32 1st Ring Road, Qingyang, Chengdu, Sichuan 610064, P.R. China
E-mail: lvchuanzhu677@126.com

Dr Guo-Sheng Zhao, Department of Spine Surgery, The Second Affiliated Hospital of Chongqing Medical University, 74 Linjiang Road, Yuzhong, Chongqing 400010, P.R. China
E-mail: zhao_gs123@126.com; zhaoguosheng@cqmu.edu.cn

[*]Contributed equally

Abbreviations: FOSL1, FOS-like antigen 1; FRA1, FOS-related antigen 1; OS, osteosarcoma; OSCs, OS stem cells; IHC, immunohistochemistry; SOX2, SRY (sex determining region Y)-box 2; siRNA, small interfering RNA; shRNA, short hairpin RNA; H&E, hematoxylin and eosin; ChIP, chromatin immunoprecipitation; IF, immunofluorescence; ECM, extracellular matrix

Key words: FOSL1, OS, stemness, anoikis resistance, SOX2

Introduction

Recent evidence suggests that primary bone cancer is a major health problem among children (0-14 years) and adolescents (15-19 years), comprising the third leading cause of cancer-related death in children and adolescents in the United

States and the sixth in China (1,2). Among primary bone cancers, osteosarcoma (OS), an aggressive malignant tumor, which is commonly accompanied by lung metastasis, is the most frequently occurring type (3). Since the 1980s, surgical removal combined with neoadjuvant chemotherapy has been the mainstay of OS treatment, significantly improving patient prognosis. However, OS treatment has not been significantly improved since then and patients with relapsed or primary metastatic OS still have a dismal prognosis, with a five-year survival rate of only 20% (4,5). Moreover, to date, no targeted therapy for OS has been approved by the US Food and Drug Agency (6). Thus, novel effective therapies for OS are urgently required.

Cancer stem cells are a small subpopulation of cancer cells that have stem-like properties and retain pluripotency and self-renewing abilities, which might be responsible for cancer metastasis or recurrence (7). Gibbs *et al* (8) first confirmed the existence of OS stem cells (OSCs) in multiple OS cell lines. Since then, OSCs have been revealed to drive OS initiation, metastasis and recurrence; therefore, targeting these cells is considered a novel and attractive strategy to treat OS (9). Several signaling pathways and genes were found to participate in the regulation of the biological function of OSCs (10). However, to date, no treatment has been approved to deplete OSCs. Thus, new biomarkers and an improved understanding of the molecular biology of OSCs are needed to develop targeted therapy to treat OS and improve patient prognosis.

Tumor metastasis results from a complex series steps, including local migration and invasion, circulation of live cancer cells, arrest at the secondary site, and tumor initiation (11). However, due to the lack of survival signals generated from the extracellular matrix (ECM) and neighboring cells, most of the cancer cells undergo apoptosis when they are detached from the ECM during circulation (12). This kind of programmed cell death, comprising apoptosis upon cell detachment from the ECM, is called anoikis (13). Anoikis is not only an important process to prevent normal cells from colonizing the wrong site in the body, but also provides a strong barrier against cancer metastasis (14). Thus, in addition to tumor initiation caused by OSCs, anoikis resistance, which prevents the key fraction of tumor cells from undergoing apoptosis and cell death during circulation, is another major cause of tumor metastasis (15). Recent studies, including our own, have provided some insights into anoikis resistance in OS (16,17). Nevertheless, the molecular mechanisms underlying anoikis resistance in OS remain incompletely understood.

FOS like antigen 1 (FOSL1), also known as FOS related antigen 1 (FRA1), is a transcription factor and a member of the activator protein 1 (AP1) complex, localizing to the cell nucleus and cytoplasm (18,19). FOSL1 can bind to the 12-O-tetradecanoylphorbol-13-acetate response element (TRE; TGAC/GTCA), a specific DNA sequence on the promoter or enhancer of its target genes, thereby mediating multiple tumor cell malignant phenotypes, such as cell migration, differentiation, apoptosis and proliferation (19). Previous evidence suggests that FOSL1 could be a candidate for targeted therapy for cancer stem cells in some types of cancer, such as head and neck squamous cell carcinoma, glioma and colorectal cancer (18,20,21). In addition, FOSL1 has been reported to be involved in K-Ras-transformed canine renal cell anoikis resistance (22). Moreover, FOSL1 mRNA was reported to be highly expressed in OS tissues, suggesting FOSL1 as a potential therapeutic target for OS (23). However, the function of FOSL1 in OS remains poorly understood and its role in maintaining cancer stemness and regulating anoikis resistance in OS is unclear.

In the present study, it was demonstrated that FOSL1 is highly expressed in OSCs and facilitates their stem-like properties, tumorigenic potential and anoikis resistance. Mechanistically, FOSL1 exerts these functions by directly promoting SOX2 (encoding SRY-box transcription factor 2) transcription. The present study highlights the important role of FOSL1 in maintaining OS cell stemness properties and anoikis resistance, suggesting FOSL1 as a promising target in OS.

Materials and methods

Cell culture. The OS cell lines 143B and MNNG/HOS were purchased from the American Type Culture Collection and maintained in Dulbecco's modified Eagle's medium (DMEM, Gibco; Thermo Fisher Scientific, Inc.) supplemented with 10% fetal bovine serum (FBS), 100 μg/ml penicillin and 100 μg/ml streptomycin. All cells were incubated at 37˚C in a humidified atmosphere containing 5% CO_2. OS spheres were cultured in 6-well ultra-low attachment plates (Corning, Inc.) in stem cell medium, which consisted of serum-free DMEM with BASIC Ham's F-12 Nutrient Mix (DMEM/F12) medium (Gibco; Thermo Fisher Scientific, Inc.) with 20 ng/ml epidermal growth factor (EGF, PeproTech, Inc.), 20 ng/ml basic fibroblast growth factor (bFGF, PeproTech, Inc.) and 2 mg/ml B27 (Gibco; Thermo Fisher Scientific, Inc.). The medium was added at 1 ml every two days during anchorage-independent proliferation.

RNA sequencing (RNA-seq) and bioinformatic analysis. Total RNA was extracted using TRIzol reagent (cat. no. 15596018CN; Thermo Fisher Scientific, Inc.) following the manufacturer's proctocol. RNA quantity and purity were analysis of Bioanalyzer 2100 and RNA 6000 Nano LabChip kit (cat. no. 5067-1511; Agilent Technologies, Inc.), high-quality RNA samples with RIN number >7.0 were used to construct sequencing library. Then, RNA-sequencing library preparation and sequencing were performed on the Illumina Novaseqä 6000 platform by LC-Bio Technology Co., Ltd. The average insert size for the final cDNA librarys were 300±50 bp. At last, the 2x150 bp paired-end sequencing (PE150) was performed on an Illumina Novaseq™ 6000 (LC-Bio Technology CO., Ltd.) following the supplier's recommended protocol. Moreover, to get high quality clean reads, reads were further filtered by Cutadapt (https://cutadapt.readthedocs.io/en/stable/). Then, the raw reads were filtered and the clean reads were mapped using HISAT2. Differential gene expression analysis was performed using DESeq2 software (https://support.bioconductor.org/tag/DESeq2/) between two different groups. The genes with parameters of a false discovery rate <0.05 and absolute fold change ≥2 were considered as differentially expressed genes (DEGs). The DEGs were then subjected to enrichment analysis for gene ontology (GO) functions and Kyoto Encyclopedia of Genes and Genomes

pathways. The raw sequence data have been submitted to the NCBI Short Read Archive (SRA) datasets with the accession number <PRJNA1080098>. For the bioinformatic analysis, the UALCAN database (https://ualcan.path.uab.edu/) (24), the R2: Genomics Analysis and Visualization Platform (https://hgserver1.amc.nl) (25), the TARGET database (using the TNMplot.com tool (https://tnmplot.com/analysis/)) (26) and the KM-plotter Platform (http://kmplot.com/) (27) were used according to the supplier's instructions.

Reverse transcription-quantitative PCR (RT-qPCR) and western blot analysis. Western blotting and RT-qPCR analyses were performed as previously described (5,17). The primers used in the present study were obtained from Sangon Biotech Co., Ltd. and are listed in Table SI. For western blotting, proteins (35 μg/lane) were separated using 8-12% SDS Tris-glycine gels and transferred onto PVDF membranes. Membranes were blocked with 5% fat-free milk for 2 h at room temperature and incubated with the appropriate primary antibodies overnight at 4˚C. Antibodies against GAPDH (1:1,000; cat. no. 60004-1-lg) were purchased from Proteintech Group, Inc. Rabbit anti-human FRA1 (1:1,000; cat. no. 252421), rabbit anti-human SOX2 (1:1,000; cat. no. 92494), rabbit anti-human NANOG (1:1,000; cat. no. 109250), rabbit anti-human BAX (1:1,000; cat. no. 32503), rabbit anti-human Caspase3 (1:1,000; cat. no. 32351) and anti-cleaved Caspase3 antibodies (1:500; cat. no. 32042) were purchased from Abcam. Rabbit anti-human BCL-2 (1:1,000; cat. no. 15071) antibodies were purchased from Cell Signaling Technology, Inc. Then, the secondary antibody (goat anti-rabbit or mouse IgG; 1:5,000; cat. nos. bs-0295G-HRP and bs-0368G-HRP; BIOSS) was applied. Immunoreactivity was detected using an ECL Kit (Beyotime Institute of Biotechnology).

Multiplex immunohistochemistry (mIHC) staining, immunohistochemistry (IHC), immunofluorescence (IF) and Transwell assays. The mIHC staining was based on the Tyramine Signal Amplification (TSA) technology, as previously described (28) and was detected by using a TSA Fluorescence Triple Staining kit (cat. no. AFIHC024; AiFang biological; http://afantibody.cn/). Other assays were performed as previously described (5,29).

IHC was performed using an IHC kit (Zsbio). Sample sections were deparaffinized through a series of xylene baths, antigens were retrieved by steam treatment in 10 mM citrate buffer, blocked with 3% hydrogen peroxide for 15 min at 37˚C, pre-incubated with blocking goat serum solution (cat. no. ZLI-9022; Zsbio) for 30 min at 37˚C, and then incubated at 4˚C with the primary antibodies overnight. Subsequently, the ready-to-use undiluted secondary antibodies conjugated with HRP in the ElivisionTM plus Polyer HRP (Mouse/Rabbit) IHC kit (cat. no. KIT-9902; Fuzhou Maixin Biotech Co., Ltd.) were applied for 40 min at 37˚C and the nuclei were counterstained with haematoxylin. The slides were then examined from non-overlapping cells using a light microscope (Olympus Corporation). Primary rabbit anti-human FRA1 (1:100, cat. no. 252421; Abcam), mouse anti-human SOX2 (1:100, cat. no. 171380; Abcam), and ready-to-use mouse anti-human c-Kit (CD117) (cat. no. kit-0029; Fuzhou Maixin Biotech Co., Ltd.) were used.

For IF, after different interventions, 143B and MNNG/HOS cells ($5x10^5$ cells per well) were fixed with 10% formalin and incubated with 0.2% Triton X-100 in PBS for 10 min followed by 5% bovine serum albumin (cat. no. GC305010; Wuhan Servicebio Technology Co., Ltd.) for 60 min at room temperature. The slides were then incubated with rabbit anti-FRA1 antibody (1:100) and mouse anti-SOX2 antibody (1:100; cat. no. 171380; Abcam) at 4˚C overnight. After washing with PBS, the slides were incubated with the corresponding secondary antibody for 60 min at room temperature. Slides were stained with nuclear dye 4,6-diamidino-2-phenylindole (DAPI; 5 μg/ml; cat. no. C1002; Beyotime Institute of Biotechnology) and cover-slipped, and FL images were captured using a fluorescence microscope (CKX53; Olympus Corporation).

For the Transwell migration assay, cells ($4x10^5$ cells/ml) were resuspended in DMEM without serum and 200 μl of the cell suspension seeded into the upper chamber of 8-μm Transwell filters (Merck KGaA). DMEM containing 15% FBS was added to the lower chambers (24-well plate) and the cells were incubated 16 h for the migration assay at 37˚C in 5% CO_2. The migratory cells were quantified after 0.1% crystal violet staining for 5 min at room temperature in five randomly selected fields (magnification, x200) under an inverted phase-contrast light microscope (Olympus Corporation).

Lentiviral transfection. The pHBLV-CMV-MCS-EF1-puro lentiviral vector for overexpressing FOSL1 and the control were synthesized and obtained from Hanbio Biotechnology Co., Ltd. The coding sequence of FOSL1 was amplified using the following primers: Forward, 5'-TACTAGAGGATCTAT TTCCGGTGAATTCGCCACCATGTTCCGAGACT-3' and reverse, 5'-GAGCGATCGCAGATCCTTAGGATCCTCACA AAGCGAGGAGGGTTG-3'. The short hairpin RNA (shRNA) in the pHBLV-U6-MCS-PGK-BSD lentiviral vector targeting SOX2 and a scrambled sequence were also purchased from Hanbio Biotechnology Co., Ltd. 293T cells were transfected with the plasmids using Lipofiter™ (cat. no. HB-TRCF-1000; Hanbio Biotechnology Co., Ltd.), in accordance with the manufacturer's protocol. After 48 and 72 h the lentiviral were vectors were collected. When 143B and MNNG/HOS cells' confluence reached 30-40%, they were infected with the lentiviral vectors according to the manufacturer's protocol [The multiplicity of infection (MOI) for h-FOSL1 and h-SOX2 shRNA lentiviral vector in OS cell lines were 40 and 20] for 24 h at 37˚C in 5% CO_2 and then cultured with puromycin (1 μg/ml for 1 week) and blasticidin (2 μg/ml for 4 days) at 37˚C in 5% CO_2 as necessary to establish stable cell lines. The subsequent experimentation began after one-time cell passage. The shRNA target sequences are listed in Table SII.

Transfection of short interfering RNA (siRNA). A total of two siRNAs targeting FOSL1 were used for the knockdown experiments (Guangzhou RiboBio Co., Ltd.). Cells were transfected with 20 nM targeting siRNA (two sequences) or scrambled siRNA, using the RiboBio-FECT™ CP kit (Guangzhou RiboBio Co., Ltd.), according to the manufacturer's protocol at 37˚C in 5% CO_2. The knockdown efficiency was assessed using RT-qPCR and western blot analysis of cells at 48 h after

transfection. The siRNA target sequences were siRNA-1, GTC GAAGGCCTTGTGAACA; and siRNA2, GGAAGGAAC TGACCGACTT.

Spheroid formation assay and plate colony formation assay. To evaluate the cells' self-renewal capacity, tumor sphere formation and colony formation assays were used. 143B and MNNG/HOS cells were cultured in stem cell medium in 96-well ultra-low attachment plates (Corning Inc.). In total, 20 or 40 cells were seeded into each well, which was supplemented with 20 μl of new stem cell medium every two days. Spheres with a size >50 μm were obtained and counted. After 10-12 days of culture, culture wells with spheres were marked and spheres were counted (30). For the plate cloning experiment, cells were seeded at a density of 50-200 cells/per well in a regular 6-well plate and cultured in a 5% CO_2 incubator at 37˚C. The medium was changed every 3 days. After observing that the proliferation of the cells had stopped, the cells were washed with phosphate-buffered saline (PBS) three times, fixed using 4% paraformaldehyde for 15 min at room temperature and stained with 0.1% crystal violet for 5 min at room temperature. Colonies with a size >50 μm were obtained and counted.

Fluorescence activated cell sorting (FACS) analysis. 143B and MNNG/HOS cells were seeded into ultra-low attachment 6-well plates to culture stem cells and then transfected with lentivirus or siRNAs as required. Cells were dissociated into single cells using Accutase (MilliporeSigma) as required, and incubated with anti-CD117 (also known as KIT proto-oncogene, receptor tyrosine kinase)-Phycoerythrin (PE)-Cyanine 7 (Cy7) antibodies (1:25; cat. no. 25-1178-42; Thermo Fisher Scientific, Inc.) and anti-Stro1-Allophycocyanin (APC) (1:100; cat. no. MA5-28635; Thermo Fisher Scientific, Inc.) antibodies, or isotype control antibodies, at 37˚C in the dark for 20 min. After staining, the cells were washed with PBS and then measured using a flow cytometer (BD FACS CantoTM II; BD Biosciences) to detect $CD117^+$ and $Stro1^+$ sub-populations.

Anoikis analysis. Cell anoikis was assessed using Annexin V-fluorescein isothiocyanate (FITC)/propidium iodide (PI) analysis as in our previous study (17). Briefly, an Annexin V-FITC/PI kit (cat. no. 556547; BD Biosciences) was used according to the manufacturer's protocols. After the cells were subjected to lentivirus or siRNA transfection, they were seeded in ultra-low attachment 6-well plates (Corning Inc.) and cultured for 24 or 48 h in DMEM supplemented with 5% FBS. Thereafter, the cells were harvested and washed, and an anti-FITC antibody and anti-PI antibody, in a 3:100 ratio with 1X buffer, were used to stain the cells in the dark for 15 min. Then, 400 μl of 1X buffer was added, and the cells were assessed using a flow cytometer (BD biosciences) with FlowJo software (version 10.8.1; BD FACS CantoTM II; FlowJo LLC). Annexin V-FITC positive, meanwhile PI negative cells and both Annexin V-FITC and PI positive cells were identified as anoikis cells.

Chromatin immunoprecipitation (ChIP)-qPCR. Chromatin immunoprecipitation coupled with qPCR was performed as described previously (20). Briefly, MNNG/HOS cells were firstly transfected with FOSL1-overexpression lentivirus and the efficiency of transfection was confirmed. Then, cells were fixed using 1% formaldehyde for 10 min at room temperature with rotation, and then quenched using glycine. Total cell lysates were sonicated to generate 200-1,000-bp DNA fragments. Chromatin complexes were immunoprecipitated following the instructions of the SimpleChIP® Enzymatic Chromatin IP Kit (cat. no. 9003; Cell Signaling Technology, Inc.) with an anti-FRA1 (FOSL1) antibody (cat. no. sc-28310; Santa Cruz Biotechnology, Inc.). The precipitated DNA samples were quantified using qPCR. Data are expressed as the percentage of input DNA. The ChIP-qPCR assays were performed in triplicate and the data are presented as the mean ± SD. The SOX2 ChIP-qPCR primers were obtained from MDL Biotech Co., Ltd. and are listed in Table SIII.

Dual-luciferase reporter assays. To create the luciferase reporter gene, the sequence of NANOG or SOX2 containing the predicted and mutated binding sites was inserted into the vector psi-CHECK2. These constructs, which included SOX2-WT (wild-type), SOX2-MT (mutated), NANOG-WT and NANOG-Mut, were synthesized by Bomaide Gene Technology Co., Ltd. The detailed sequences are listed Tables SIV and SV. In brief, cells were first seeded in 6-well plates and cultured to 60-80% confluency. Then, Lipofectamine 2000 (Invitrogen; Thermo Fisher Scientific, Inc.) was used to co-transfect the luciferase reporter gene with either over-FOSL1 or NC plasmids (Biomed) into MNNG/HOS cells. At 48 h after transfection, *Firefly* and *Renilla* luciferase activities in each well were detected using the Dual Luciferase Reporter Gene Assay kit (Shanghai Yeasen Biotechnology Co., Ltd.) according to the manufacturer's protocol.

Animals. A total of 95 female (4 weeks-old) athymic BALB/c nude mice (weight, 18-20 g) were obtained from Vital River Laboratory Animal Technology Co., Ltd. Housing conditions included temperature (22±2˚C), humidity (40-60%), 12/12-h light/dark cycle and feed *ad libitum* to minimize the distress of animals. No mouse succumbed before euthanasia; and all the mice were euthanized by inhaling 40% CO_2, with a flow rate of 5 l/min for 5 min, using a carbon dioxide inhalation device and followed by 5 min monitoring to verify irreversible euthanasia before they were sacrificed; and the fill rate of carbon dioxide was standardized by the experimental animal division of Chongqing Medical University. Animal death is typically verified by checking for absence of respiration and heartbeat. All the animal care and experimental procedures were approved (approval no. 2022-224) by the Institutional Animal Care and Use Committee of the Second Affiliated Hospital of Chongqing Medical University (Chongqing, China), and were performed according to the Guide for the Care Use of Laboratory Animals.

Xenografts and tumor initiation assays in vivo. Xenograft models were generated as previously reported (5) and 25 mice were randomly divided into 5 groups (n=5 mice in each group). Briefly, MNNG/HOS cell suspensions ($2x10^7$ cells/ml) in PBS were injected subcutaneously into each mouse in a volume of 0.1 ml. The mice health and weight were monitored every two days and xenografts were observed and measured

every three days. The volume of the xenografts was calculated as V (mm^3)=1/2 x (length x $width^2$) (31). All the mice were sacrificed at 20 or 24 days after injection and tumors were harvested and measured. The xenografts were fixed, sectioned, subjected to haematoxylin and eosin (H&E) staining, and further analyzed using IHC. The tumor initiation assay was carried out using a limiting-dilution assay in the aforementioned mice xenograft models with the injection of different low doses ($5x10^3$, 10^4, $5x10^4$ and $5x10^5$) of MNNG/HOS OSCs and 40 mice were divided into 5 groups (one mouse carried two doses of OSCs). The tumor re-initiating cell frequency of OSCs was calculated using the ELDA software (http://bioinf.wehi.edu.au/software/elda/) (32).

In vivo anoikis and lung metastasis model. The lung metastasis models were established as previously reported (5,17) and 30 mice were randomly divided into 5 groups (n=6 mice in each group). Briefly, to emphasize the influence of anoikis, with appropriate treatments, fewer cells ($2x10^6$) in a volume of 100 μl PBS were injected into the tail vein of each 4-week-old nude mouse. Mice health and weight were monitored every two days. Then all the mice were sacrificed at 20 days after injection. All the lungs were resected and fixed. Then, the fixed lungs were embedded in paraffin, sectioned and stained with H&E, followed by counting the microscopic lung metastases and determining the metastasis rate.

Statistical analysis. Quantitative data are presented as the mean ± SD and were analyzed using unpaired Student's t-tests or the Mann-Whitney test (non-parametric test when the P-value of the F test was <0.05) for two groups. One-way ANOVA analysis with Tukey's multiple comparisons was used for comparisons among three or more groups. All analyses were performed using GraphPad Prism (version 8.00, GraphPad Software, Inc.; Dotmatics). *In vitro* functional experiments were performed at least in triplicate.

Results

FOSL1 expression is upregulated in OSCs and is associated with the stem cell-like phenotype of OS cells. Previously, FOSL1 was reported to be highly expressed in human OS tissues compared with that in non-tumor tissues (23). To further confirm this, a pan-cancer analysis was first applied by analyzing The Cancer Genome Atlas samples at the UALCAN database to examine the FOSL1 expression in multiple human benign tissues and tumors (Fig. 1A). A higher rate of abnormal FOSL1 expression was observed in multiple cancers, including sarcoma, with a relatively high abundance. Then, by analyzing the TARGET database, it was observed that compared with that in normal bones, FOSL1 expression was significantly upregulated in OS tissues (Fig. 1B). Moreover, survival analysis revealed that high expression of FOSL1 was significantly associated with lower overall survival and disease-free survival in sarcoma (Fig. 1C). Together, these bioinformatic findings suggested that FOSL1 had a potential oncogenic role in OS.

Recent evidence suggested that FOSL1 could be a candidate for targeted therapy for cancer stem cells (21) and OSCs were considered to be the cause of tumor formation, recurrence and metastasis (9). Therefore, it was decided to investigate whether FOSL1 plays a critical role in OSCs. Firstly, OS-spheres were cultured in a serum-free medium supplied with cytokines to enrich OSCs (30) (Fig. S1A). In addition, to confirm the enrichment of OSCs, FACS analysis demonstrated that the population of $CD117^+$ and Stro-1^+ cells, which have been proven as surface markers of OSCs (33), were significantly increased and the expression levels of stemness-related transcription factors SOX2 and NANOG were significantly upregulated, following OS-sphere culture (Fig. S1B-D). Thereafter, RNA-seq was employed to analyze the dynamic gene expression patterns during acquisition of the stem-like properties by OS cells (five samples for each group). The results are demonstrated in Fig. 1D-F. Notch, Hedgehog and AP-1 pathways which have been widely used to study the maintenance of OS or other cancer cell stemness (10,34,35) are activated. Thus, the differential expression of the major genes of these signaling pathways was then explored and it was found that FOSL1 expression was significantly increased during acquisition of the stem-like properties in OS cells, which was confirmed using RT-qPCR and western blotting (Fig. 1G-I). More importantly, in the IF analysis, besides upregulation of FOSL1 protein levels, FOSL1 was mostly located in the nucleus (Fig. 1J). FOSL1 is a transcription factor; therefore, these data suggested that FOSL1 might be involved in the biological function of OSCs.

To validate the functional role of the upregulated expression of FOSL1 in OSCs, two siRNAs (siRNA-1 and siRNA-2) were generated to target two different FOSL1 sequences. Both siRNAs were able to knockdown FOSL1 expression in 143B and MNNG/HOS OS cell lines (Fig. 2A). As revealed in Fig. 2A-D, depletion of FOSL1 significantly inhibited the tumor sphere and colony formation ability of OS cells, and reduced the protein levels of SOX2 and NANOG in 143B and MNNG/HOS cells. In addition, knockdown of FOSL1 significantly reduced the number of $CD117^+$ and Stro-1^+ cells (Fig. 2E). These results suggested that FOSL1 is involved in regulating the self-renewal and stemness phenotype of OSCs. Collectively, the present data suggested that FOSL1 is significantly upregulated and is a potential regulator of the stemness phenotype of OSCs.

FOSL1 maintains OSC stemness and promotes anoikis resistance in OS. To further address whether FOSL1 promotes the stemness phenotype and self-renewal ability in OS *in vitro*, FOSL1 was stably overexpressed using the lentivirus-based overFOSL1 plasmid in 143B and MNNG/HOS cells and the effect was examined using western blotting (Fig. 3A). Then, *in vitro* tumor sphere formation and colony formation assays were performed to detect the self-renewal ability in OS cells. Unsurprisingly, the sphere-forming and colony formation capacity of FOSL1-overexpressing cells was significantly increased compared with that in the overexpression control (overCon) cells, and the spheres generated from FOSL1-overexpressing cells were markedly bigger than those generated from overCon cells (Fig. 3B-D). Subsequently, it was found that overFOSL1 OS cells had significantly higher protein levels of SOX2 and NANOG compared with overCon OS cells (Fig. 3A). In addition, FACS analysis demonstrated that the population of $CD117^+$ and Stro-1^+ OS cells was significantly increased following FOSL1 overexpression in 143B

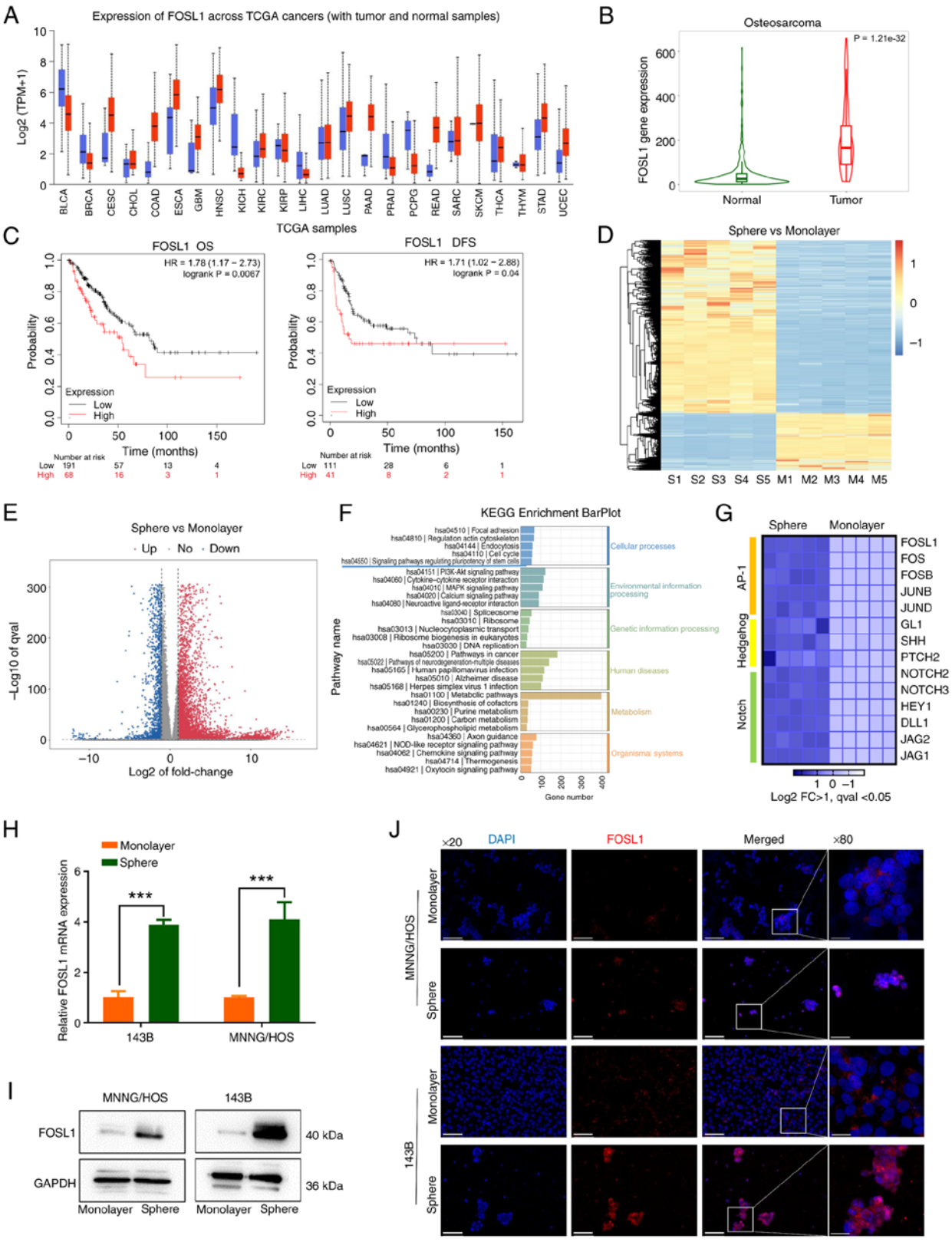

Figure 1. FOSL1 is highly expressed in OS and upregulated in OSCs. (A) Expression of FOSL1 across a pan-cancer analysis in TCGA samples, as analyzed at the UALCAN cancer database (https://ualcan.path.uab.edu/). (B) The expression of FOSL1 in OS tissues (red) and normal samples (green) in the TARGET database, assessed using the TNMplot.com tool (https://tnmplot.com/analysis/). (C) Kaplan-Meier curves of FOSL1 expression related to overall survival and disease-free survival in sarcoma in the TCGA database, analyzed using the KM-plotter database (https://kmplot.com/analysis/). (D and E) The heat map and volcano map of the RNA-seq data, between monolayer groups (adherent cells) and sphere groups (rich in OSCs). n=5, Log2|FC| >1, qval <0.05. (F) KEGG Enrichment BarPlot of the RNA-seq data. (G) Heat map of the differentially expressed genes in the Notch, AP-1, and Hedgehog pathways, from gene expression profiling results based on the RNA-seq data. n=5, Log2|FC| >1, qval <0.05. (H) The mRNA expression of FOSL1 in tumor sphere cells compared with that in monolayer adherent cells, in the indicated cell lines. ***P<0.001. (I) FOSL1 expression patterns in the indicated groups according to western blotting in 143B and MNNG/HOS cells. (J) The difference in the distribution and expression of FOSL1 in the monolayer and sphere groups of OS cell lines (143B and MNNG/HOS) as analyzed using immunofluorescence staining, Scale bars, 100 μm for the x20 images and 25 μm for the x80 images. OS, osteosarcoma; OSCs, OS stem cells; FOSL1, FOS-like antigen 1; TCGA, The Cancer Genome Atlas; KEGG, Kyoto Encyclopedia of Genes and Genomes.

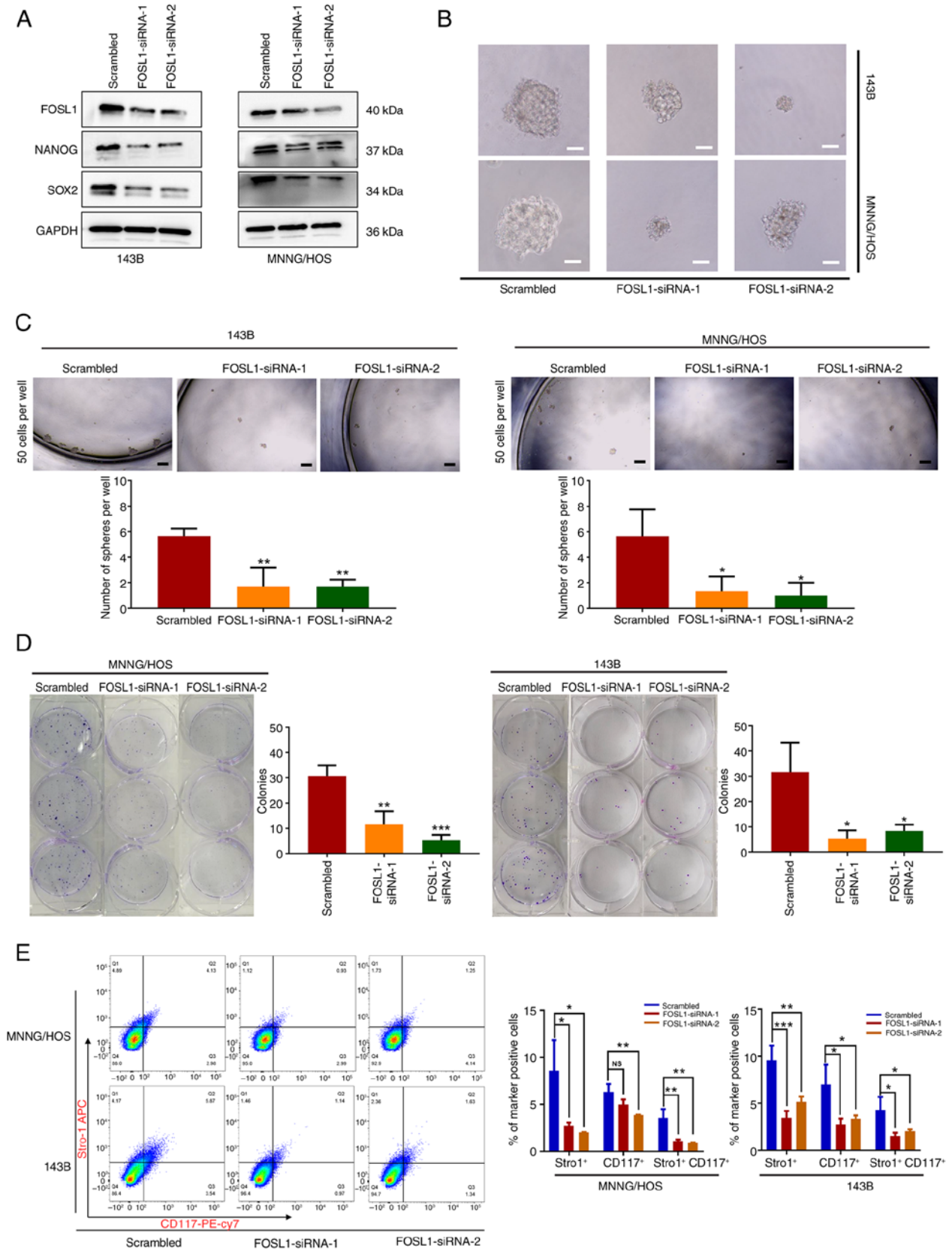

Figure 2. Upregulated expression of FOSL1 in OSCs is associated with the maintenance of stem-like properties. (A) Representative images of western blot analysis of FOS1L, NANOG and SOX2 levels in 143B and MNNG/HOS cells, following transfection with two siRNAs targeting FOSL1. (B) Results of a sphere formation test of OSC stemness after transfection with siRNA-FOSL1. Typical photomicrographs of the newly formed clonal spheres are shown. Scale bars, 50 μm. (C) Statistical analysis of the numbers of clonal spheres. scale bars, 100 μm. (D) Transfection with siRNA-FOSL1 attenuated colony-formation by OS cell lines (143B and MNNG/HOS). Images of colony formation captured after 12 days of culture for 143B cells or 13 days of culture for MNNG/HOS cells. (E) Results of flow cytometric analysis carried out to measure CD117 and Stro1 expression on 143B and MNNG/HOS OS cells (after suspension culture) following transfection with siRNA-FOSL1. Each experiment was conducted three times. *P<0.05, **P<0.01 and ***P<0.001 compared with the scrambled group. FOSL1, FOS-like antigen 1; OS, osteosarcoma; OSCs, OS stem cells; SOX-2, SRY (sex determining region Y)-box 2; siRNA, small interfering RNA; NS, not significant (P>0.05).

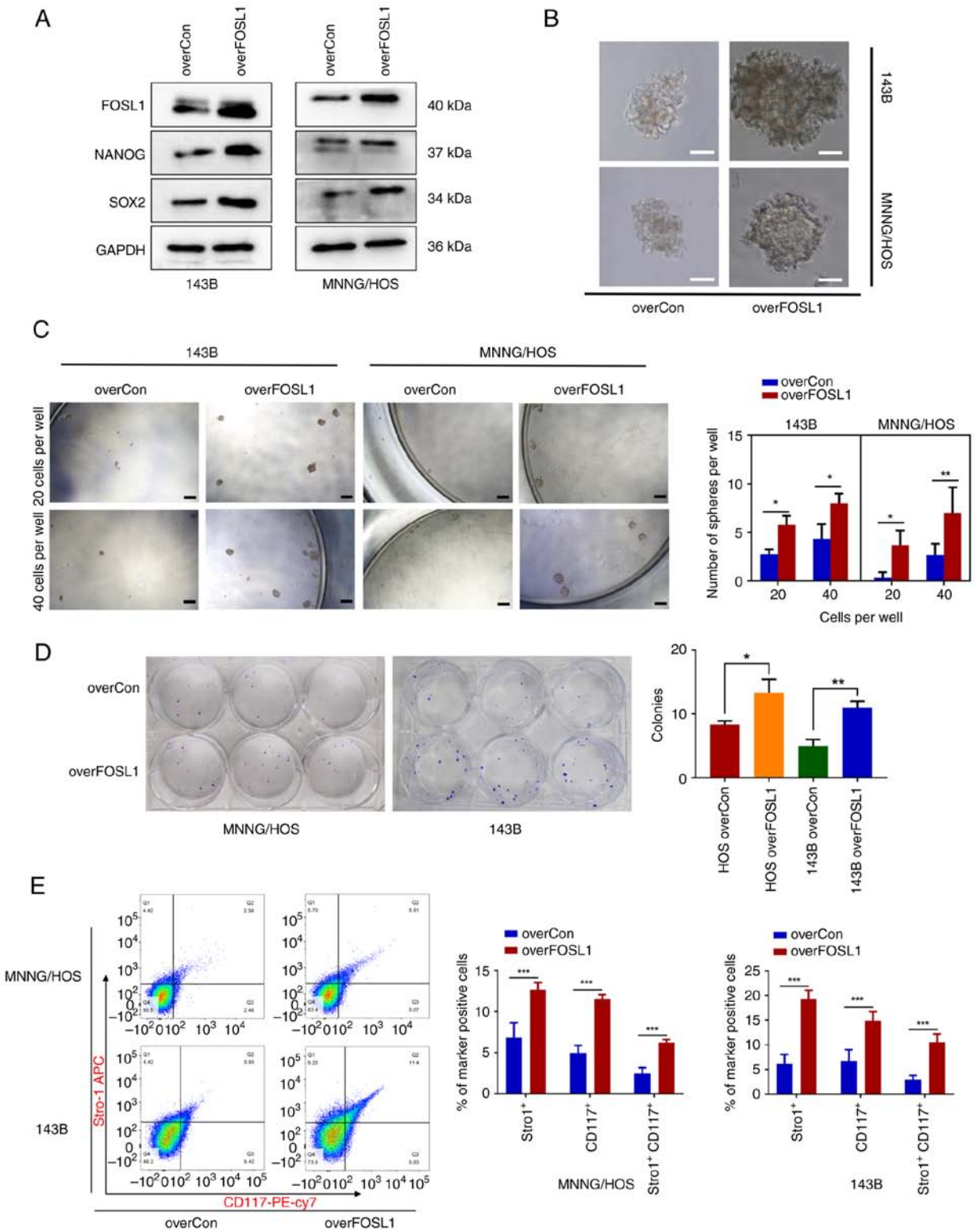

Figure 3. Overexpression of FOSL1 enhances the stem-like properties of OS cells. (A) Representative images of western blot analysis of FOS1L, NANOG and SOX2 levels in 143B and MNNG/HOS cells treated with or without FOSL1-overexpression. (B) Typical photomicrographs of the newly formed clonal spheres after overexpression of FOSL1 or not. Scale bars, 50 μm. (C) Statistical analysis of the numbers of clonal spheres at two cell seeding densities (20 or 40 per well). Scale bars, 100 μm. (D) Results of colony formation assays in OS cell lines (143B and MNNG/HOS) overexpressing FOSL1. Images of colony formation were captured after 14 days of culture. (E) Flow cytometric analysis of CD117 and Stro1 expression on 143B and MNNG/HOS OS cells (after suspension culture), with or without FOSL1-overexpression. Each experiment was conducted three times. *P<0.05, **P<0.01 and ***P<0.001. FOSL1, FOS-like antigen 1; OS, osteosarcoma; SOX-2, SRY (sex determining region Y)-box 2; overCon, overexpression control.

and MNNG/HOS sphere cells (Fig. 3E). Thus, these findings confirmed that FOSL1 is a key regulator that promotes the stemness phenotype of OS *in vitro*.

Metastasis is a major factor that predicts poor prognosis in patients with OS (36). High expression of FOSL1 is considered to facilitate the metastasis of malignant tumors of

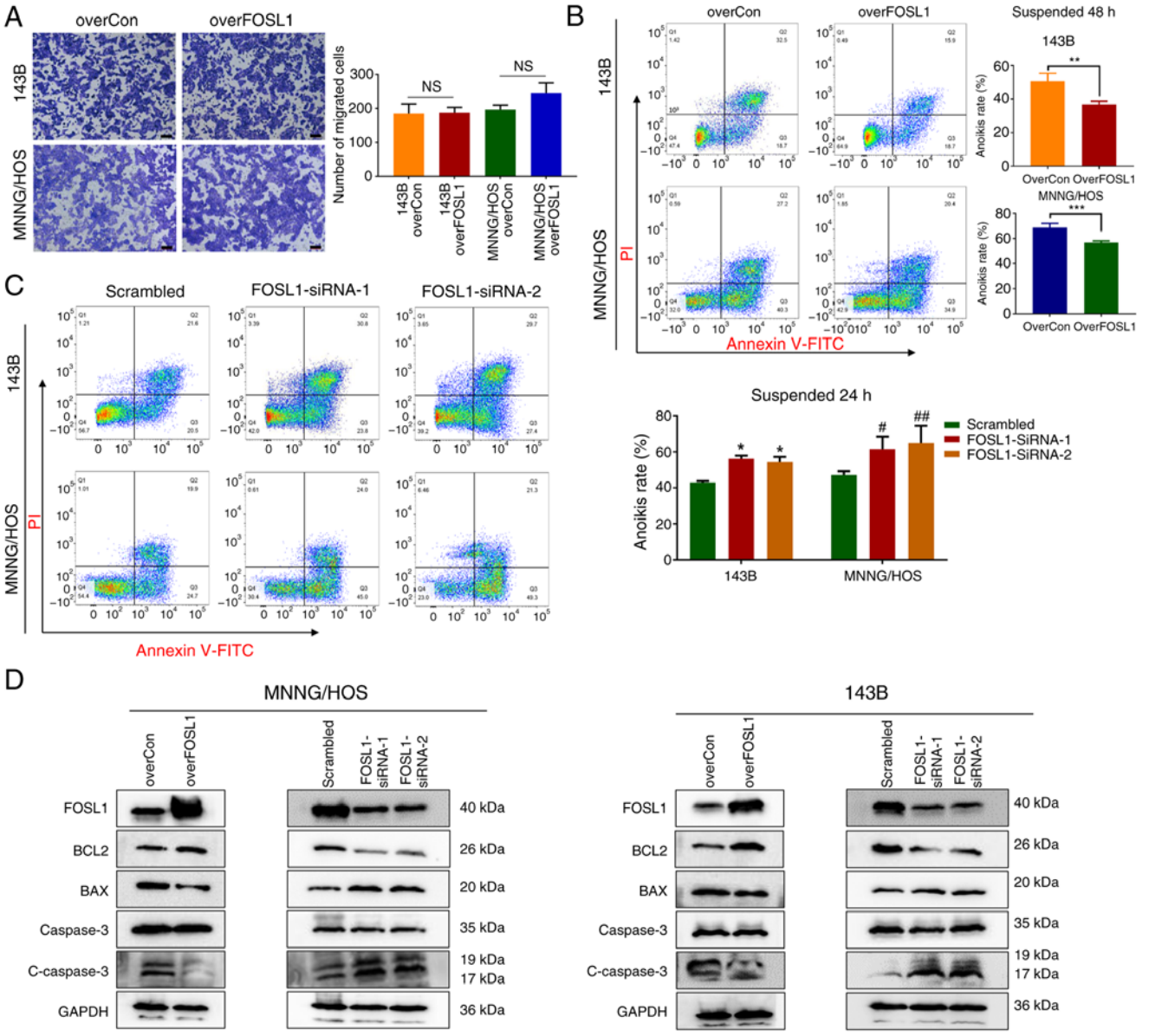

Figure 4. Crucial involvement of FOSL1 expression in OS cells anoikis resistance. (A) Representative images and statistical analysis of the Transwell assay of cells overexpressing FOSL1 or not. Scale bars, 50 μm. (B) Results of an Annexin V-FITC/PI assay for the anoikis rates in the overCon and overFOSL1 (FOSL1 overexpression) groups of OS cell lines 143B and MNNG/HOS after incubation for 48 h. **P<0.01 and ***P<0.001. (C) Results of Annexin V-FITC/PI assays for the anoikis rates in the indicated groups transfected with siRNA-FOSL1, after suspension culture for 24 h. *P<0.05 compared with the 143B scrambled group; $^{\#}$P<0.05 and $^{\#\#}$P<0.01, compared with the MNNG/HOS scrambled group. (D) Representative images of the western blot analysis for FOSL1, BCL2, BAX, Caspase 3 and cleaved-Caspase 3 in 143B and MNNG/HOS cells. Cells were subjected to FOSL1 overexpression or silencing. FOSL1, FOS-like antigen 1; OS, osteosarcoma; NS, not significant (P>0.05); overCon, overexpression control; siRNA, small interfering RNA.

epithelial origin by promoting their migration and invasion ability (18,37); however, the relationship between FOSL1 and OS metastasis is unclear. To examine the effect of FOSL1 in regulating OS cell metastasis *in vitro*, Transwell assays were first performed to determine whether the change in FOSL1 expression influenced the migration ability of OS cells. Surprisingly, FOSL1 overexpression did not have a significant effect on the migration of 143B and MNNG/HOS cells (Fig. 4A). While searching for other possible mechanisms by which FOSL1 might regulate OS cell metastasis, our attention was drawn to anoikis resistance, which is an important process in tumor distant metastasis (17,38). A previous study identified that FOSL1 is involved in regulating anoikis resistance in the K-Ras transformed Madin-Darby Canine Kidney (MDCK) cell line (23). Thus, it was investigated whether FOSL1 could affect anoikis in OS cells using ultra-low attachment 6-well plates to create suspension conditions. After suspension culture for 24 or 48 h, it was found that overexpression of FOSL1 significantly attenuated the anoikis rate compared with their respective control group, and an increased percentage of anoikis cells was observed after transfection with FOSL1 siRNAs in 143B and MNNG/HOS cells (Fig. 4B and C). Consequently, the dynamic changes in the levels of apoptotic proteins were detected. The results demonstrated that overexpression of FOSL1 not only increased anti-apoptotic protein B-cell CLL/lymphoma 2 (BCL2) expression, but also reduced the levels of pro-apoptotic protein BCL2 associated X protein (BAX) and cleaved Caspase-3 in the 143B and MNNG/HOS

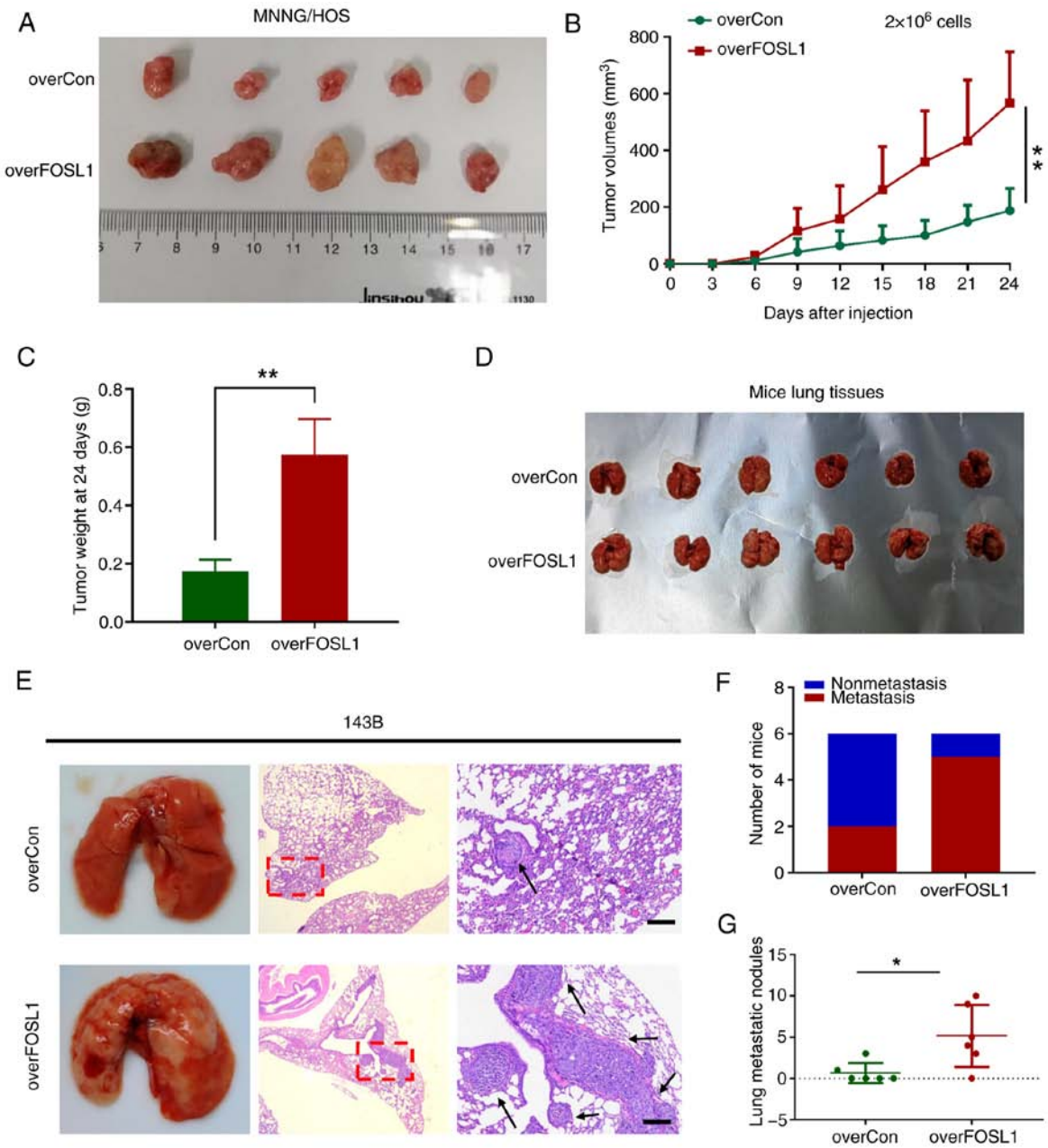

Figure 5. FOSL1 facilitates osteosarcoma cell tumorigenesis and lung metastasis *in vivo*. (A) Representative MNNG/HOS xenograft tumors excised at the end of the experiment from sacrificed nude mice with the indicated treatments. (B and C) Growth curves and tumor weight of the subcutaneous xenograft tumors. **P<0.01. (D) Macroscopic images of the mouse lungs as indicated. (E) Representative macroscopic and microscopic images (H&E staining) of the mouse lungs, as indicated. The red dotted line area was enlarged and red arrows indicate potential metastatic lesions. Scale bars, 100 μm. (F) Percentage of mice bearing lung metastases in each group (n=6). (G) Statistical analysis of the number of lung metastatic nodules quantified on a lung H&E stained section. *P<0.05, Mann-Whitney test. FOSL1, FOS-like antigen 1; overCon, overexpression control.

cells under suspension culture, which was reversed by knockdown of FOSL1 (Fig. 4D). These results allowed us to conclude that FOSL1 could reduce anoikis sensitivity in OS cells.

FOSL1 promotes OS cell tumorigenicity and metastasis in vivo. Having shown that FOSL1 could promote the stemness phenotype and anoikis resistance in OS cells *in vitro*, it was important to determine whether these effects could also be detected *in vivo*. Subcutaneous xenograft models were created with 2x10^6 tumor cells inoculated subcutaneously into athymic nude mice after treatment with or without FOSL1 overexpression. In addition, an *in vivo* limiting-dilution assay with the subcutaneous xenograft models was performed with two different low doses (5x10^4 and 5x10^5) of overFOSL1-MNNG/HOS cells and their corresponding control cells. In agreement with the *in vitro* results, FOSL1-MNNG/HOS cells displayed significantly higher tumorigenicity and tumor re-initiating cell frequency compared with those of the control cells (Fig. S2). Moreover, FOSL1 overexpression significantly increased OS growth, as reflected by the tumor size, volume and tumor weight of the xenograft tumors (Fig. 5A-C).

Anoikis resistance, as well as extensive self-renewal potential, are both critical factors that drive tumor cell metastasis (39).

To further investigate whether FOSL1-induced anoikis resistance and stemness promotion contribute to metastasis *in vivo*, a mouse lung metastasis model was applied by injecting OS cells into the tail vein. In line with our *in vitro* findings, it was demonstrated that overexpression of FOSL1 significantly increased the ability of 143B cells to produce lung metastases compared with that of the control cells, as reflected by the increased metastasis incidence and number of OS metastatic nodules in the lungs (Fig. 5D-G). Thus, the *in vitro* and *in vivo* results indicated that FOSL1 plays as a crucial role in facilitating the tumorigenesis and metastasis of OS by promoting the stemness potential and anoikis resistance of OS cells.

FOSL1 upregulates SOX2 expression by interacting with the SOX2 promoter and activating its transcription. Previous evidence has highlighted FOSL1 as a versatile transcription factor, with numerous biological roles (40). As demonstrated in Fig. 6A, after transfection with the lentivirus-based overFOSL1 plasmid, FOSL1 expression was significantly upregulated. Notably, FOSL1 was localized in the nucleus of 143B and MNNG/HOS cells, indicating its active role as a transcription factor. To identify the key downstream factor promoting the OS stemness phenotype controlled by FOSL1, the R2 database was further analyzed to investigate the correlation between FOSL1 and some key stemness transcription factors in OS samples (9,41). The results revealed that there was a positive correlation between FOSL1 and SOX2 ($r=0.322$, $P<0.001$) (Fig. 6B). It was shown that overexpression of FOSL1 could upregulate SOX2 protein levels. To further confirm the regulation at the mRNA level, RT-qPCR was performed. The results verified that overexpression of FOSL1 significantly and consistently increased the mRNA expression levels of SOX2 in the two OS cell lines (Fig. 6C). Based on the aforementioned results, it would be expected that overexpression of FOSL1 would enhance SOX2 promoter activity. To confirm this hypothesis, FOSL1 or the negative control were transiently overexpressed in MNNG/HOS cells cotransfected with the SOX2 promoter-luciferase construct and then a dual luciferase assay was performed. As expected, SOX2 transcriptional activity was increased after FOSL1 overexpression. In addition, the potential binding site sequence between FOSL1 and the SOX2 promoter might be 'ATGACACACC', because the promotion effect of FOSL1 disappeared after the SOX2 promoter was mutated at this site (Fig. 6D and Table SII). Similar results were obtained using ChIP coupled with RT-qPCR, which confirmed that in overFOSL1 MNNG/HOS cells, FOSL1 could strongly bind to the SOX2 promoter, highlighting that SOX2 is a target of FOSL1 (Fig. 6E). Moreover, mIHC staining and IF assays showed colocalization of FOSL1 and SOX2 proteins in overFOSL1 MNNG/HOS xenograft tumor tissues and overFOSL1 OS cells (Fig. 6F and G). These results also suggested an interaction between FOSL1 and SOX2 in OS cells. Additionally, given that NANOG has been reported as a target gene of FOSL1 (21) and its protein expression was upregulated in OS cells after FOSL1 overexpression, RT-qPCR and luciferase reporter assays were applied to investigate whether NANOG is also a candidate transcriptional target gene of FOSL1. In contrast to previous results, overexpression of FOSL1 only improved the mRNA expression levels of NANOG in MNNG/HOS cell line but not obvious in the 143B cell line, and although FOSL1 activated the transcription of NANOG in MNNG/HOS cells, the increase was not obvious (Fig. 6C and D). Thus, wit is considered that in OS cells, SOX2 is more likely to be the key downstream target of FOSL1, rather than NANOG. Taken together, the results indicated that SOX2 is a major transcriptional target of FOSL1 in OS cells.

SOX2 contributes to the FOSL1-promoted stemness phenotype and anoikis resistance in OS cells. SOX2 was reported to be a key protein related to the maintenance of a stem-like phenotype in several type of tumors, including OS (42). Thus, to determine whether the FOSL1-promoted stemness phenotype of OS cells was related to SOX2, SOX2 expression was knocked down using shRNA lentiviruses (two sequences), which were transfected into FOSL1-overexpressing cells, with western blot analysis confirming this result (Fig. 7A). It was found that knockdown of SOX2 significantly abrogated FOSL1 overexpression-induced promotion of sphere formation and colony formation in 143B and MNNG/HOS cells (Fig. 7B-D). Subsequently, it was found that knockdown of SOX2 also attenuated the FOSL1 overexpression-induced increase in the population of $CD117^+$ and Stro-1^+ OS cells among 143B and MNNG/HOS cells, as assessed using FACS assays (Fig. 7E). These data indicated that FOSL1 promotion of the self-renewal ability of OS cell lines is related to SOX2.

Moreover, compared with the extensive research on cell stemness maintenance, relatively little attention had been paid to SOX2 in the field of cell resistance to anoikis. A recent study reported that SOX2 could also be a driver of the acquisition of anoikis resistance in ovarian carcinoma cells (43). However, the exact role of SOX2 in the regulation of anoikis in OS remains unclear. Therefore, to investigate whether SOX2 contributes to the FOSL1-induced suppression of anoikis in OS cells, shSOX2-1 and shSOX2-2 lentiviruses were used to eliminate the upregulated expression of SOX2 after transfection with the FOSL1-overexpression lentiviruses. As shown in Fig. 8A-C, as expected, after anchorage-independent suspension culture, overexpression of FOSL1 significantly reduced the anoikis rate of 143B and MNNG/HOS cells, while the anoikis rates were partly restored after knockdown of SOX2. This was consistent with the change in the anoikis rate induced by the FOSL1 overexpression-mediated increase in BCL2 protein levels, and the reduction of BAX and cleaved Caspase-3 protein levels in OS cells under the aforementioned suspension culture conditions, which was also partially reversed by knockdown of SOX2 (Fig. 8D). These data demonstrated that SOX2 is necessary for FOSL1-induced promotion of the stemness phenotype and anoikis resistance in OS.

Targeting SOX2 inhibits FOSL1-associated promotion of tumorigenesis and metastasis in OS. To further investigate whether SOX2 contributes to FOSL1-induced promotion of tumorigenesis and metastasis in OS *in vivo*, subcutaneous xenograft models were first established by stably transfecting overFOSL1 MNNG/HOS cells, with or without shSOX2, into nude mice. An *in vivo* limiting-dilution assay with the subcutaneous xenograft models was first performed with four different low doses ($5x10^3$, 10^4, $5x10^4$ and $5x10^5$) of cells. Interestingly, the tumorigenicity and tumor re-initiating cell frequency in the overFOSL1 group was increased compared with those in the control group, but were significantly reduced after knockdown of SOX2 (Fig. 9A-C). Moreover, the FOSL1-induced increase

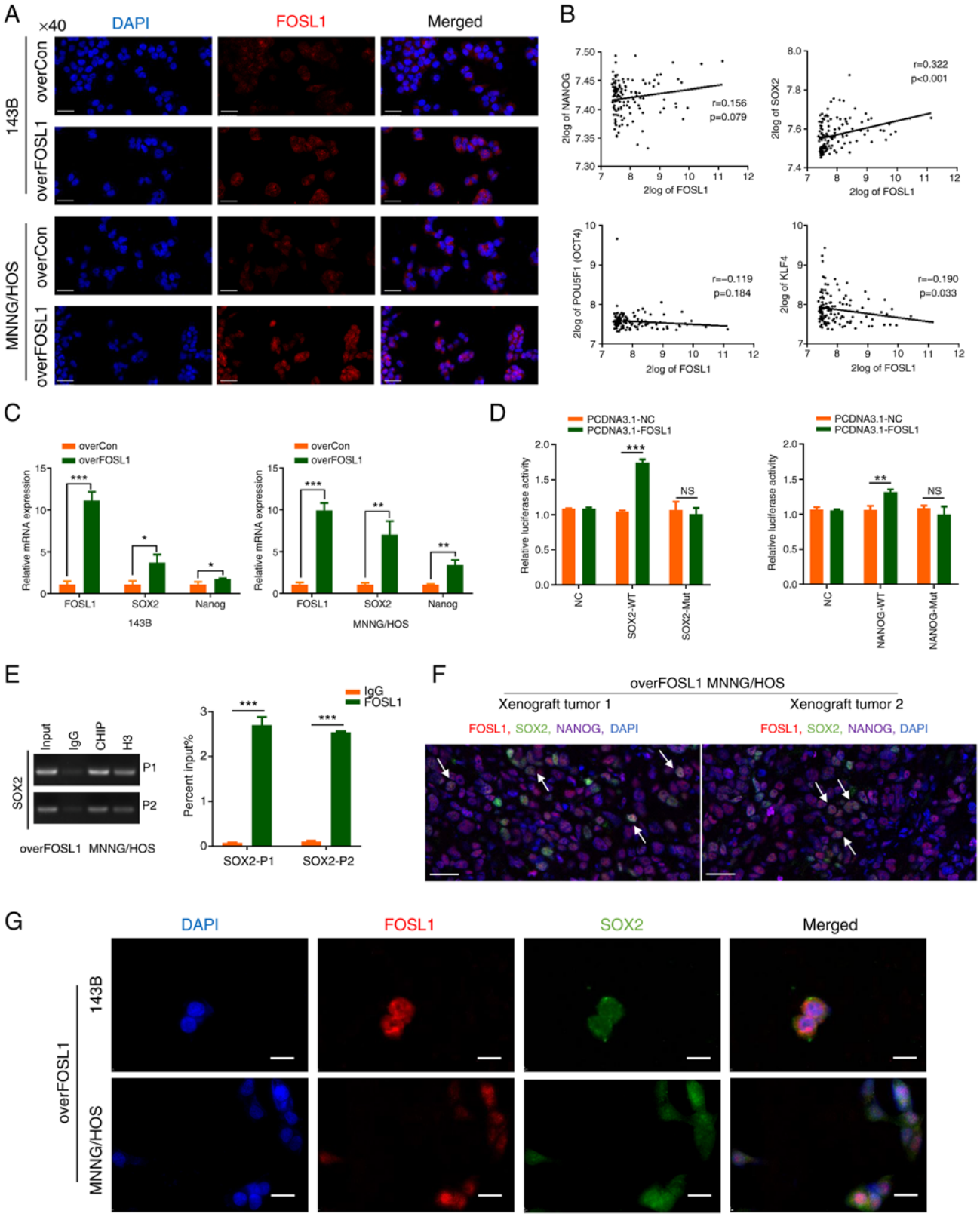

Figure 6. FOSL1 upregulates SOX2 expression by promoting SOX2 transcriptional activation. (A) Immunofluorescence staining showing the difference in the distribution and expression of FOSL1 in monolayer OS cell lines (143B and MNNG/HOS) after overexpression of FOSL1. Scale bars, 50 μm. (B) Pearson correlation analysis between FOSL1 and stemness transcription factor expression levels carried out at the R2 OS gene expression database (http://hgserver1.amc.nl) using the dataset named mixed OS-Kuijjer-127-vst-ilmnhwg6v2. (C) The mRNA expression levels of FOSL1, SOX2 and NANOG after overexpression of FOSL1 in the indicated cell lines. (D) Luciferase activity of MNNG/HOS cells transformed with a luciferase reporter plasmid expressing WT SOX2 or NANOG and Mut SOX2 or NANOG, co-transfected with PCDNA3.1-FOSL1 or the negative control. (E) The enrichment in the FOSL1, IgG (negative control) and H3 (positive control) groups at the SOX2 promoter in overFOSL1 (FOSL1 overexpression) MNNG/HOS cells, as detected using a ChIP-PCR assay. (F) Multiplex immunohistochemistry staining using the TSA assay for the xenograft tumor tissues of overFOSL1 MNNG/HOS cells. Markers were used as indicated. scale bars: 25 μm. (G) Subcellular localization of FOSL1 and SOX2 in overFOSL1 143B and MNNG/HOS cells, as analyzed using confocal laser scanning microscopy. Scale bars, 25 μm. *P<0.05, **P<0.01 and ***P<0.001. FOSL1, FOS-like antigen; SOX-2, SRY (sex determining region Y)-box 2; OS, osteosarcoma; WT, wild-type; Mut, mutant; NS, not significant (P>0.05); overCon, overexpression control.

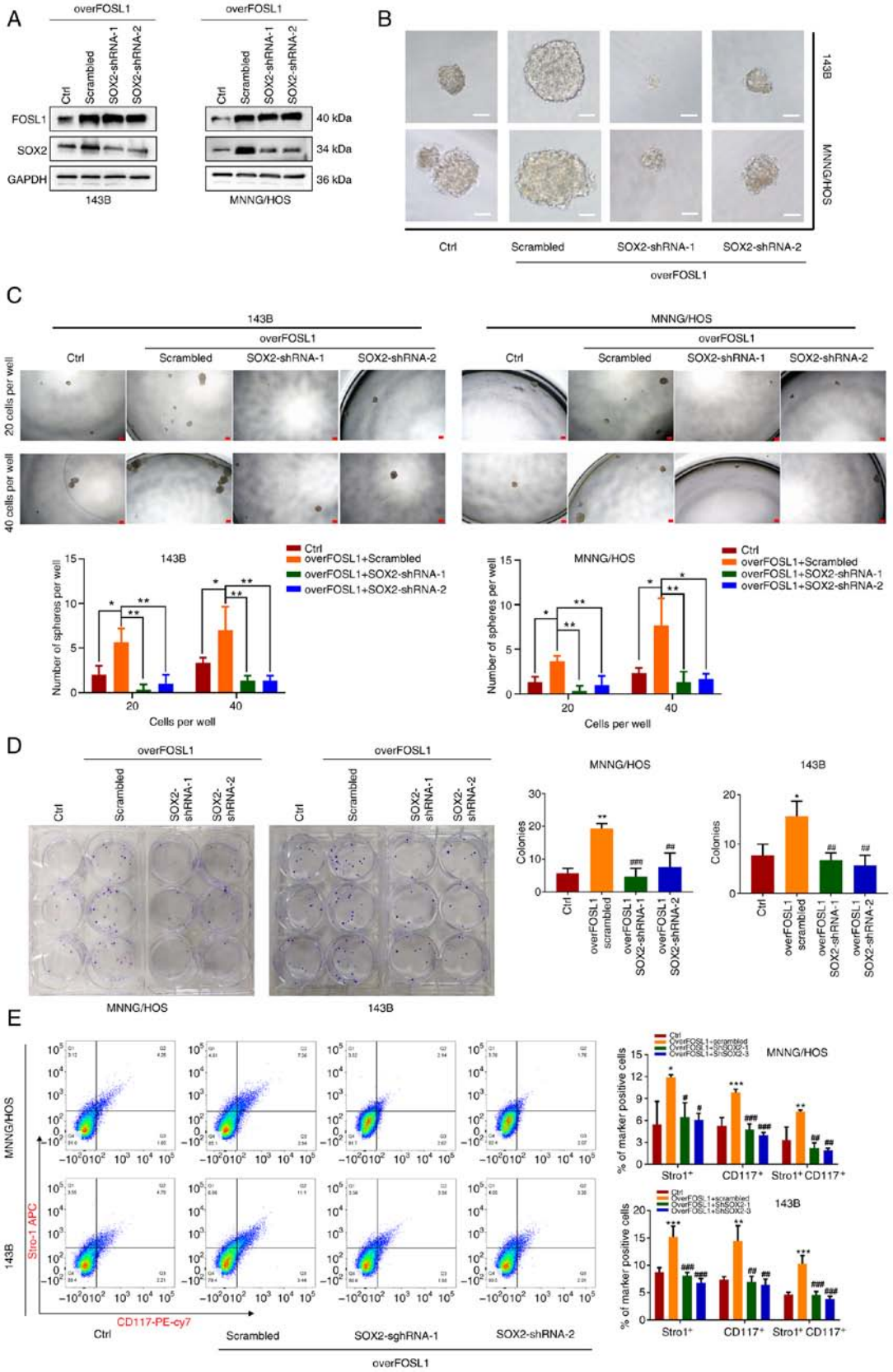

Figure 7. SOX2 is involved in FOSL1-mediated promotion of osteosarcoma stem cell features. (A) Representative images of western blot analysis of FOSL1 and SOX2 levels in 143B and MNNG/HOS cells overexpressing FOSL1 or not, with shRNA-mediated silencing of SOX2. (B) Typical photomicrographs of the newly formed clonal spheres after the cells were treated as indicated, scale bars: 50 μm. (C) Statistical analysis of the numbers of clonal spheres at two cell seeding densities (20 or 40 per well), after the cells were treated as indicated. Scale bars, 100 μm. *P<0.05 and **P<0.01. (D) Colony formation abilities of overFOSL1 (FOSL1 overexpression) and shSOX2 lentivirus-transfected143B and MNNG/HOS cell lines. Images of colony formation were captured after 14 days of culture. *P<0.05 and **P<0.01 compared with the Ctrl group; $^{\#\#}$P<0.01 and $^{\#\#\#}$P<0.001 compared with the overFOSL1 Scrambled group. (E) Flow cytometric analysis of CD117 and Stro1 expression on 143B and MNNG/HOS osteosarcoma cells (after suspension culture). Cells were treated as indicated. Each experiment was conducted three times. *P<0.05, **P<0.01 and ***P<0.001 compared with the Ctrl group; $^{\#}$P<0.05, $^{\#\#}$P<0.01 and $^{\#\#\#}$P<0.001; compared with the overFOSL1 Scrambled group. SOX-2, SRY (sex determining region Y)-box 2; FOSL1, FOS-like antigen; shRNA, short hairpin RNA.

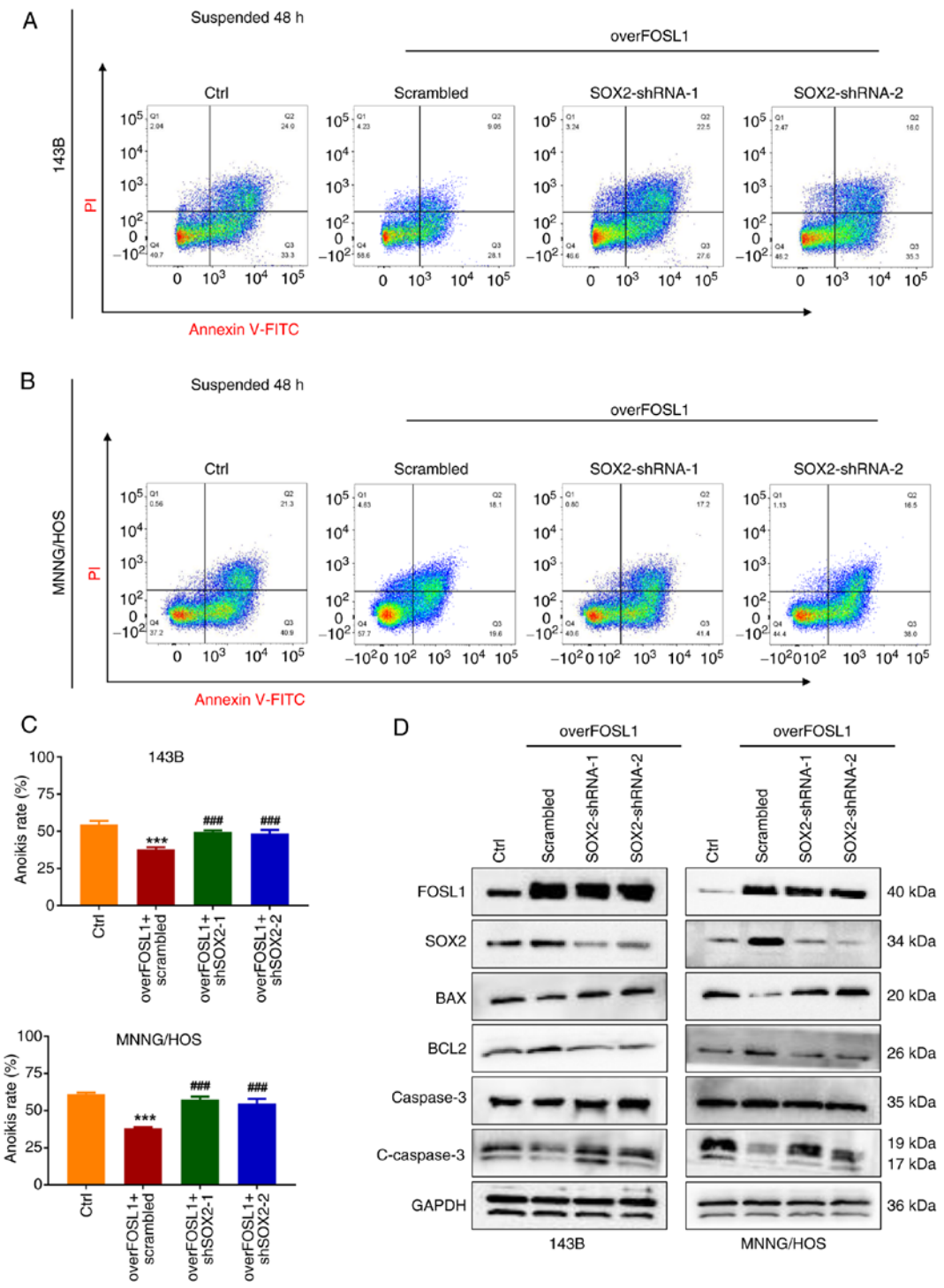

Figure 8. SOX2 is required for FOSL1-mediated promotion of the anoikis resistant properties of OS cells. (A and B) The anoikis rates were detected by an Annexin V-FITC/PI assay in the four groups of OS cell lines 143B and MNNG/HOS, as indicated, after suspension culture for 48 h. (C) The statistical analysis of the quantitative flow cytometry data in A and B. ***P<0.001 compared with the Ctrl group; $^{###}$P<0.001 compared with overFOSL1 (FOSL1 overexpression) and scrambled group. (D) Representative images of the western blot analysis of FOSL1, SOX2, BCL2, BAX, Caspase 3 and cleaved-Caspase 3 in 143B and MNNG/HOS cells. Cells were subjected to FOSL1 overexpression and SOX2 silencing, as indicated. SOX-2, SRY (sex determining region Y)-box 2; FOSL1, FOS-like antigen; OS, osteosarcoma; shRNA, short hairpin RNA.

in OS growth ability *in vivo* was also reduced after knockdown of SOX2 (Fig. S3). In addition, the fact that overexpression of FOSL1 enhanced SOX2 expression and knockdown of SOX2 decreased its protein expression were further confirmed *in vivo* using IHC staining for FOSL1 and SOX2 proteins in mouse xenograft tumor tissues (Fig. 9D). As expected, the rate of positive CD117 IHC staining was low in the control groups, significantly increased in the FOSL1-overexpressing group, and reduced in the FOSL1-overexpressing + SOX2-knockdown group, suggesting that SOX2 contributes to FOSL1-induced promotion of stemness and tumorigenesis *in vivo* (Fig. 9D). Consistent with our *in vitro* findings, it was found that FOSL1 could significantly increase the ability of OS cells to produce lung metastases compared with that of the control

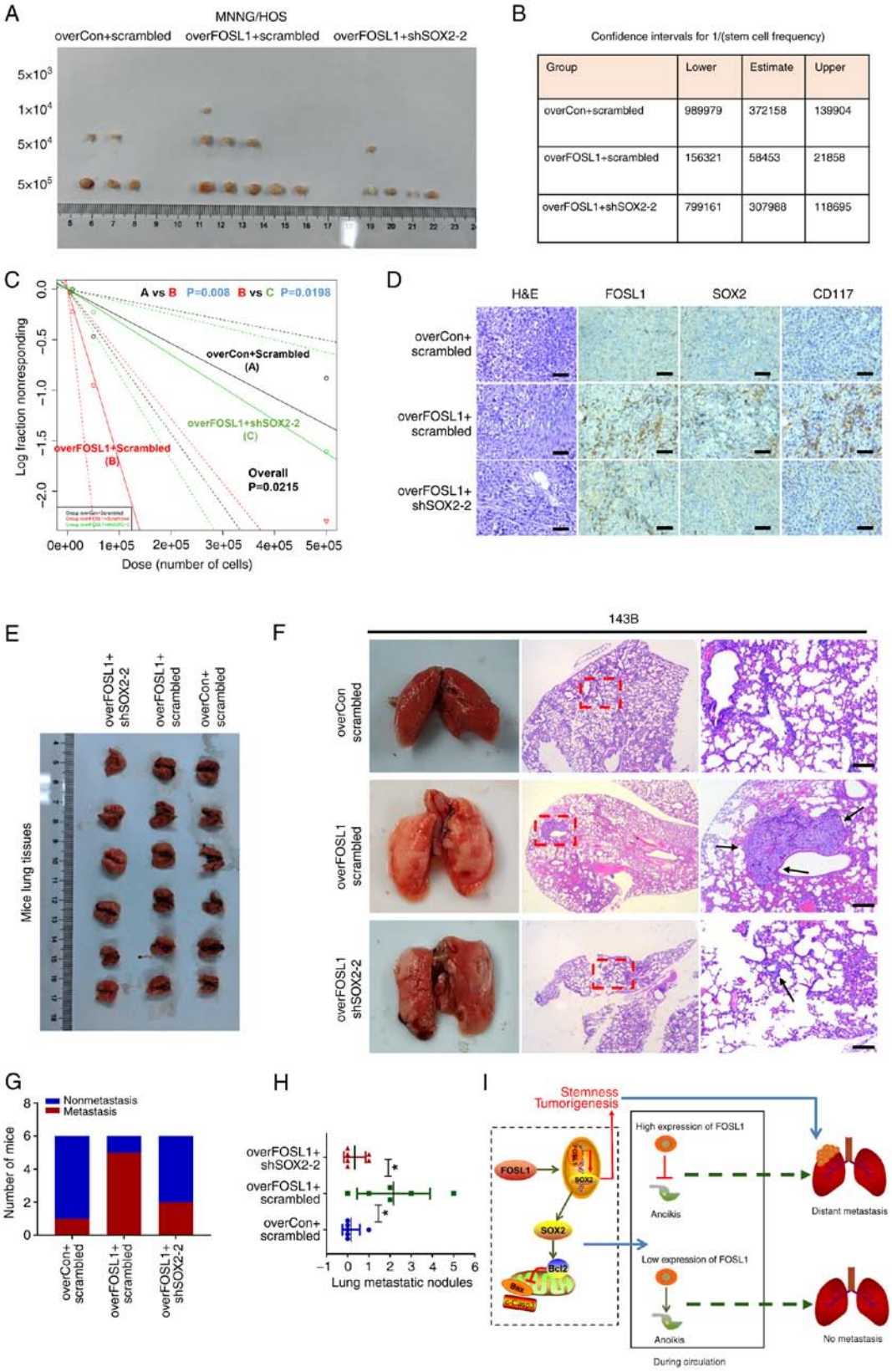

Figure 9. SOX2 contributes to FOSL1-induced facilitation of tumorigenesis and lung metastasis *in vivo*. (A) *In vivo* limiting dilution analysis of the indicated groups of cells. (B) The confidence intervals for 1/(stem cell frequency) in the three indicated groups, generated using the ELDA software (http://bioinf.wehi.edu.au/software/elda/index.html). (C) The tumor re-initiating cell frequency of the three indicated groups; frequency and probability estimates were computed using the ELDA software. (D) Confirmation of the effect of FOSL1-overexpression and SOX2 knockdown on the stemness of OS cells *in vivo* using CD117 immunohistochemical staining. Scale bars, 50 μm. (E) Macroscopic images of the mice lungs as indicated. (F) Representative macroscopic and microscopic images (H&E staining) of mouse lungs as indicated. The red dotted line area was enlarged and black arrows indicate confirmed metastatic lesions. Scale bars, 100 μm. (G and H) Percentage of the mice bearing lung metastases in each group (n=6) and the statistical analysis of lung metastatic nodules quantified on a lung H&E stained section. *P<0.05. (I) Schematic model illustrating how FOSL1 regulates stem-cell phenotype and anoikis resistance of OS and the role of SOX2 in FOSL1-induced promotion of tumorigenesis and lung metastasis. SOX-2, SRY (sex determining region Y)-box 2; FOSL1, FOS-like antigen; OS, osteosarcoma; overCon, overexpression control.

cells. However, knockdown of SOX2 reduced the ability of FOSL1-overexpressing cells to establish lung metastases, as reflected by the decreased metastasis incidence and number of OS metastatic nodules in the lungs compared with those in the overFOSL1 group (Fig. 9 E-H). These results, together with our *in vitro* findings, highlighted a functional role for FOSL1 and SOX2 in the regulation of tumorigenesis and metastasis in OS (Fig. 9I).

Discussion

Considering that OS treatment has not significantly improved over the past 40 years, there is an urgent clinical need to develop novel and effective treatments for this common sarcoma (29). Although the average 5-year survival rate of patients with OS has increased to ~65% (1), the survival rate reduces markedly in patients with overt metastases (4). Indeed, the main reason for poor prognosis of OS can be attributed to metastases. Therefore, there is a pressing need to find an effective therapy to reduce OS metastasis. Emerging evidence suggests that cancer stem cells cause cancer metastasis, local recurrence and therapy resistance in multiple types of cancer, including OS (7,10,44). Theoretically, according to their tumor initiation ability, OSCs are considered as important 'seeds', which enter the blood circulation and initiate colonization at the secondary site, thus forming a distant metastasis. However, most circulating cancer cells will be eliminated during blood circulation; therefore, an anoikis resistance ability is needed to allow the surviving cells to eventually reach the secondary site of metastasis (11). Thus, metastasis formation is considered to be restricted to, and driven by, a rare subpopulation of tumor cells with a distinctive set of characteristics, including resistance to anoikis and extensive self-renewal potential (39). Interestingly, Guha *et al* (45) found that anoikis-resistant cancer cells exhibited similar biological characteristics to cancer stem cells, reflecting that these cells can express high levels of cancer stem cell biomarkers such as CD44, CD133, OCT4, NANOG and SOX2. Thus, it was aimed to identify a collective target for OSCs and anoikis resistance to provide a new insight into OS therapy. Accordingly, in the present study, it was demonstrated that FOSL1 could be a new target, not only for OSCs, but also for anoikis resistance in OS cells.

FOSL1, as a component of the activated protein-1 (AP-1) transcription factor complex, has been reported as a key regulator that maintains stem cell-like characteristics in various cancers, such as glioblastoma (46), head and neck squamous cell carcinoma (18) and colorectal cancer (21). However, the functional role of FOSL1 in OS is infrequently discussed and remains poorly understood. In the present study, the role of FOSL1 was investigated in OS and OSCs. In agreement with the results of a previous study (23), it was found that FOSL1 mRNA expression was upregulated in OS tissues compared with that in normal tissues, and might be a predictor for poor prognosis in patients with sarcomas. Previous evidence suggests that overexpression of different AP-1 complex members could induce genesis of OS in immortalized human mesenchymal stem cells and exhibited an OS phenotype, indicating a process of tumor initiation (35). OSCs are tumor initiation cells and FOSL1 is a member of the AP-1 complex, acting as a stemness regulator in other kinds of cancers; therefore, it was hypothesized that FOSL1 could also regulate the OS stemness phenotype. As expected, based on the RNA-seq results, it was found that numerous AP-1 related genes were upregulated in OSCs, including FOSL1. Confirmatory experiments demonstrated that the FOSL1 protein level is upregulated in OSCs and importantly, depletion of FOSL1 severely attenuated the self-renewal ability of OSCs. Consistent with our hypothesis, studies have suggested that silencing FOSL1 expression using RNA interference is a promising option to deplete cancer stem cells (18,47). Moreover, it was revealed that overexpression of FOSL1 not only promoted the self-renewal ability and stemness biomarker expression levels (CD117, Stro-1, SOX2 and NANOG) in OS cells, but also decreased their anoikis rate. Indeed, the effect of FOSL1 in facilitating lung metastasis was confirmed using the mouse tail vein model to simulate anoikis. Accumulating evidence has highlighted the importance of triggering the integrin pathway and suppressing intrinsic pathways to avoid anoikis (13,17). Zhang *et al* (22) found that FOSL1 could upregulate α6-integrin expression in K-Ras^{V12}-transformed MDCK cells. Thus, western blot analysis was used to clarify the relationship between FOSL1 and BCL-2 family proteins, which are the common downstream targets for the integrin pathway during anoikis regulation. Consequently, it was demonstrated that FOSL1 regulated OS cell anoikis by upregulating the anti-apoptotic protein BCL2, and decreasing BAX expression. In addition, the FOSL1-induced reduction in the occurrence of cell death observed when anchorage-dependent cells detached from the ECM might partly contribute to its promotion of an increased OSC population. Cancer stem cells are considered to have an innate ability to evade anoikis and are capable of anchorage-independent proliferation (48). Moreover, there is evidence that cancer stem cells could protect non-stem cells from anoikis (49). Thus, it is not unlikely that the increase in the proportion of OSCs could decrease the anoikis rate of OS cells. Moreover, FOSL1 was reported to facilitate tumor cell migration and invasion in various cancers (37,50). However, surprisingly, after FOSL1 overexpression, a significant effect on OS cell migration ability was not observed in two OS cell lines, which might be explained by heterogeneity among different kinds of tumors. Overall, the present findings highlight a novel role for FOSL1 as a target for OSCs and anoikis resistance in OS.

In OS, SOX2 and NANOG were both reported as key genes related to the maintenance of a stem-like phenotype (9,41) and the current findings showed that both SOX2 and NANOG protein levels are upregulated after FOSL1 overexpression. However, in contrast to the study of Wang *et al* (21) that FOSL1 plays transcriptional regulation role in NANOG expression in colorectal cancer cells, it was found that SOX2 is more likely to be a direct transcriptional target of FOSL1 in OS cells. Studies have emphasized the pluripotency-inducing transcription factor function of SOX2 in OS (9,51); therefore, our observation that SOX2 contributes to FOSL1-induced promotion of OC cell self-renewal was not unexpected. However, the function of SOX2 in anoikis resistance in OS cells remains unclear. In the present study, it was identified that SOX2 is an essential factor through which FOSL1 regulates BCL2, BAX and cleaved-Caspase 3 protein levels, thereby regulating OS cell anoikis. Unfortunately, whether BCL2 or BAX are direct

or indirect transcriptional targets of SOX2 is beyond the scope of the present study. However, consistent with the present findings, a recent study showed that SOX2 could drive the anoikis resistance ability of ovarian carcinoma cells by regulating apoptotic pathway genes (43). Moreover, another study also reported that inhibition of SOX2 could induce changes in cell apoptosis and BCL2 protein family expression through phosphatidylinositol-4,5-bisphosphate 3-kinase (PI3K)/protein kinase B (AKT) pathways in Ewing's sarcoma cells (52). Collectively, the results of the present study confirmed the crucial involvement of SOX2 in FOSL1-mediated stemness and anoikis in OS; however, future experiments should focus on gaining a more detailed understanding of the mechanism of SOX2 in the regulation of cell anoikis.

Taken together, the present data highlight the importance of FOSL1 in OSCs. Moreover, FOSL1 is an important regulator that promotes stemness and anoikis resistance to facilitate tumorigenesis and metastasis in OS. In addition, SOX2 is the direct transcriptional target of FOSL1. Thus, FOSL1 might represent an attractive target for therapeutic intervention to treat OS.

Acknowledgements

The authors would like to thank Professor Qiao-Nan Guo and Professor Yang-Fan Lv from the Xinqiao Hospital (Army Medical University) for their guidance on the present study. The authors are also grateful to the Department of Pathology of Xinqiao Hospital for providing parts of the experimental apparatus and for their assistance with immunohistochemical techniques. The authors also appreciate the support of LC Bio Technology Co., Ltd. for assisting with sequencing and/or bioinformatics analysis.

Funding

The present study was supported by the National Natural Science Foundation of China (NSFC) (grant nos. 82303465 and 82303712), the Natural Science Foundation of Chongqing, China (grant no. CSTB2022NSCQ-MSX0103), the Special Financial Aid to the Post doctor Research Project of Chongqing (grant no. 2022CQBSHTB3079) and the China Postdoctoral Science Foundation (grant no. 2023MD734132).

Availability of data and materials

The data generated in the present study may be requested from the corresponding author. The data generated in the present study may be found in the Sequence Read Archive database under accession number PRJNA1080098 or at the following URL: https://www.ncbi.nlm.nih.gov/bioproject/PRJNA1080098.

Authors' contributions

GSZ, CL and YW designed the experiments. YW, QH and GSZ participated in the whole experiment, and collected and analyzed the data. GSZ performed data analysis, prepared the figures and wrote the manuscript. YC and LY participated in the cell culture and animal experiments. YFW contributed to the bioinformatics analysis. SZ and YB provided technical and theoretical support. QH, LY and HL participated in the western blot analysis and manuscript preparation. GSZ, CL and YY provided financial and administrative support. GSZ, CL and YW confirm the authenticity of all the raw data. All authors read and approved the final version of the manuscript.

Ethics approval and consent to participate

All the animal care and experimental procedures were approved (approval no. 2022-224) by the Institutional Animal Care and Use Committee of the Second Affiliated Hospital of Chongqing Medical University (Chongqing, China), and were performed according to the Guide for the Care Use of Laboratory Animals.

Patient consent for publication

Not applicable.

Competing interests

The authors declare that they have no competing interests.

References

1. Siegel RL, Giaquinto AN and Jemal A: Cancer statistics, 2024. CA Cancer J Clin 74: 12-49, 2024.
2. Zheng R, Zhang S, Zeng H, Wang S, Sun K, Chen R, Li L, Wei W and He J: Cancer incidence and mortality in China, 2016. J Natl Cancer Cent 2: 1-9, 2022.
3. Ferguson JL and Turner SP: Bone Cancer: Diagnosis and treatment principles. Am Fam Physician 98: 205-213, 2018.
4. Mensali N, Köksal H, Joaquina S, Wernhoff P, Casey NP, Romecin P, Panisello C, Rodriguez R, Vimeux L, Juzeniene A, *et al*: ALPL-1 is a target for chimeric antigen receptor therapy in osteosarcoma. Nat Commun 14: 3375, 2023.
5. Zhao GS, Gao ZR, Zhang Q, Tang XF, Lv YF, Zhang ZS, Zhang Y, Tan QL, Peng DB, Jiang DM and Guo QN: TSSC3 promotes autophagy via inactivating the Src-mediated PI3K/Akt/mTOR pathway to suppress tumorigenesis and metastasis in osteosarcoma, and predicts a favorable prognosis. J Exp Clin Cancer Res 37: 188, 2018.
6. Kim YI, Tseng YC, Ayaz G, Wang S, Yan H, du Bois W, Yang H, Zhen T, Lee MP, Liu P, *et al*: SOX9 is a key component of RUNX2-regulated transcriptional circuitry in osteosarcoma. Cell Biosci 13: 136, 2023.
7. Zhang S, Zhu N, Li HF, Gu J, Zhang CJ, Liao DF and Qin L: The lipid rafts in cancer stem cell: A target to eradicate cancer. Stem Cell Res Ther 13: 432, 2022.
8. Gibbs CP, Kukekov VG, Reith JD, Tchigrinova O, Suslov ON, Scott EW, Ghivizzani SC, Ignatova TN and Steindler DA: Stem-like cells in bone sarcomas: Implications for tumorigenesis. Neoplasia 7: 967-976, 2005.
9. Yan GN, Lv YF and Guo QN: Advances in osteosarcoma stem cell research and opportunities for novel therapeutic targets. Cancer Lett 370: 268-274, 2016.
10. Martins-Neves SR, Sampaio-Ribeiro G and Gomes CMF: Self-Renewal and pluripotency in osteosarcoma stem cells' chemoresistance: Notch, Hedgehog, and Wnt/β-Catenin Interplay with Embryonic Markers. Int J Mol Sci 24: 8401, 2023.
11. Ullmann P, Rodriguez F, Schmitz M, Meurer SK, Qureshi-Baig K, Felten P, Ginolhac A, Antunes L, Frasquilho S, Zügel N, *et al*: The miR-371~373 cluster represses colon cancer initiation and metastatic colonization by inhibiting the TGFBR2/ID1 signaling axis. Cancer Res 78: 3793-3808, 2018.
12. Taddei ML, Giannoni E, Fiaschi T and Chiarugi P: Anoikis: An emerging hallmark in health and diseases. J Pathol 226: 380-393, 2012.
13. Paoli P, Giannoni E and Chiarugi P: Anoikis molecular pathways and its role in cancer progression. Biochim Biophys Acta 1833: 3481-3498, 2013.

14. Han YH, Wang Y, Lee SJ, Jin MH, Sun HN and Kwon T: Regulation of anoikis by extrinsic death receptor pathways. Cell Commun Signal 21: 227, 2023.
15. Sattari Fard F, Jalilzadeh N, Mehdizadeh A, Sajjadian F and Velaei K: Understanding and targeting anoikis in metastasis for cancer therapies. Cell Biol Int 47: 683-698, 2023.
16. Sun T, Zhong X, Song H, Liu J, Li J, Leung F, Lu WW and Liu ZL: Anoikis resistant mediated by FASN promoted growth and metastasis of osteosarcoma. Cell Death Dis 10: 298, 2019.
17. Zhao GS, Zhang Q, Cao Y, Wang Y, Lv YF, Zhang ZS, Zhang Y, Tan QL, Chang Y, Quan ZX, *et al*: High expression of ID1 facilitates metastasis in human osteosarcoma by regulating the sensitivity of anoikis via PI3K/AKT depended suppression of the intrinsic apoptotic signaling pathway. Am J Transl Res 11: 2117-2139, 2019.
18. Zhang M, Hoyle RG, Ma Z, Sun B, Cai W, Cai H, Xie N, Zhang Y, Hou J, Liu X, *et al*: FOSL1 promotes metastasis of head and neck squamous cell carcinoma through super-enhancer-driven transcription program. Mol Ther 29: 2583-2600, 2021.
19. Jiang X, Xie H, Dou Y, Yuan J, Zeng D and Xiao S: Expression and function of FRA1 protein in tumors. Mol Biol Rep 47: 737-752, 2020.
20. Guo S, Ramar V, Guo AA, Saafir T, Akpobiyeri H, Hudson B, Li J and Liu M: TRPM7 transactivates the FOSL1 gene through STAT3 and enhances glioma stemness. Cell Mol Life Sci 80: 270, 2023.
21. Wang T, Song P, Zhong T, Wang X, Xiang X, Liu Q, Chen H, Xia T, Liu H, Niu Y, *et al*: The inflammatory cytokine IL-6 induces FRA1 deacetylation promoting colorectal cancer stem-like properties. Oncogene 38: 4932-4947, 2019.
22. Zhang K, Myllymäki SM, Gao P, Devarajan R, Kytölä V, Nykter M, Wei GH and Manninen A: Oncogenic K-Ras upregulates ITGA6 expression via FOSL1 to induce anoikis resistance and synergizes with αV-Class integrins to promote EMT. Oncogene 36: 5681-5694, 2017.
23. Shen H, Wang W, Ni B, Zou Q, Lu H and Wang Z: Exploring the molecular mechanisms of osteosarcoma by the integrated analysis of mRNAs and miRNA microarrays. Int J Mol Med 42: 21-30, 2018.
24. Chandrashekar DS, Karthikeyan SK, Korla PK, Patel H, Shovon AR, Athar M, Netto GJ, Qin ZS, Kumar S, Manne U, *et al*: UALCAN: An update to the integrated cancer data analysis platform. Neoplasia 25: 18-27, 2022.
25. Zhao SJ, Jiang YQ, Xu NW, Li Q, Zhang Q, Wang SY, Li J, Wang YH, Zhang YL, Jiang SH, *et al*: SPARCL1 suppresses osteosarcoma metastasis and recruits macrophages by activation of canonical WNT/β-catenin signaling through stabilization of the WNT-receptor complex. Oncogene 37: 1049-1061, 2018.
26. Bartha Á and Győrffy B: TNMplot.com: A web tool for the comparison of gene expression in normal, tumor and metastatic tissues. Int J Mol Sci 22: 2622, 2021.
27. Győrffy B: Discovery and ranking of the most robust prognostic biomarkers in serous ovarian cancer. Geroscience 45: 1889-1898, 2023.
28. Yang Y, Huang H, Li L and Yang Y: Multiplex Immunohistochemistry Staining for Paraffin-embedded lung cancer tissue. J Vis Exp 2023.
29. Wang Y, Zhang L, Zhao G, Zhang Y, Zhan F, Chen Z, He T, Cao Y, Hao L, Wang Z, *et al*: Homologous targeting nanoparticles for enhanced PDT against osteosarcoma HOS cells and the related molecular mechanisms. J Nanobiotechnology 20: 83, 2022.
30. Yan GN, Tang XF, Zhang XC, He T, Huang YS, Zhang X, Meng G, Guo DY, Lv YF and Guo QN: TSSC3 represses self-renewal of osteosarcoma stem cells and Nanog expression by inhibiting the Src/Akt pathway. Oncotarget 8: 85628-85641, 2017.
31. Naito S, von Eschenbach AC, Giavazzi R and Fidler IJ: Growth and metastasis of tumor cells isolated from a human renal cell carcinoma implanted into different organs of nude mice. Cancer Res 46: 4109-4115, 1986.
32. Hu Y and Smyth GK: ELDA: Extreme limiting dilution analysis for comparing depleted and enriched populations in stem cell and other assays. J Immunol Methods 347: 70-78, 2009.
33. Adhikari AS, Agarwal N, Wood BM, Porretta C, Ruiz B, Pochampally RR and Iwakuma T: CD117 and Stro-1 identify osteosarcoma tumor-initiating cells associated with metastasis and drug resistance. Cancer Res 70: 4602-4612, 2010.
34. Marques C, Unterkircher T, Kroon P, Oldrini B, Izzo A, Dramaretska Y, Ferrarese R, Kling E, Schnell O, Nelander S, *et al*: NF1 regulates mesenchymal glioblastoma plasticity and aggressiveness through the AP-1 transcription factor FOSL1. Elife 10: e64846, 2021.
35. Gambera S, Abarrategi A, Rodríguez-Milla MA, Mulero F, Menéndez ST, Rodriguez R, Navarro S and García-Castro J: Role of Activator Protein-1 complex on the phenotype of human osteosarcomas generated from mesenchymal stem cells. Stem Cells 36: 1487-1500, 2018.
36. Whittle SB, Offer K, Roberts RD, LeBlanc A, London C, Majzner RG, Huang AY, Houghton P, Alejandro Sweet Cordero E, Grohar PJ, *et al*: Charting a path for prioritization of novel agents for clinical trials in osteosarcoma: A report from the Children's Oncology Group New Agents for Osteosarcoma Task Force. Pediatr Blood Cancer 68: e29188, 2021.
37. Hyakusoku H, Sawakuma K, Sano D, Takahashi H, Hatano T, Sato K, Isono Y, Shimada S, Takada K, Kuwahara T, *et al*: FosL1 regulates regional metastasis of head and neck squamous cell carcinoma by promoting cell migration, invasion, and proliferation. Anticancer Res 41: 3317-3326, 2021.
38. Dai Y, Zhang X, Ou Y, Zou L, Zhang D, Yang Q, Qin Y, Du X, Li W, Yuan Z, *et al*: Anoikis resistance-protagonists of breast cancer cells survive and metastasize after ECM detachment. Cell Commun Signal 21: 190, 2023.
39. Celià-Terrassa T and Kang Y: Distinctive properties of metastasis-initiating cells. Genes Dev 30: 892-908, 2016.
40. Lee BK, Uprety N, Jang YJ, Tucker SK, Rhee C, LeBlanc L, Beck S and Kim J: Fosl1 overexpression directly activates trophoblast-specific gene expression programs in embryonic stem cells. Stem Cell Res 26: 95-102, 2018.
41. Qi XT, Li YL, Zhang YQ, Xu T, Lu B, Fang L, Gao JQ, Yu LS, Zhu DF, Yang B, *et al*: KLF4 functions as an oncogene in promoting cancer stem cell-like characteristics in osteosarcoma cells. Acta Pharmacol Sin 40: 546-555, 2019.
42. Yang L, Shi P, Zhao G, Xu J, Peng W, Zhang J, Zhang G, Wang X, Dong Z, Chen F and Cui H: Targeting cancer stem cell pathways for cancer therapy. Signal Transduct Target Ther 5: 8, 2020.
43. Shonibare Z, Monavarian M, O'Connell K, Altomare D, Shelton A, Mehta S, Jaskula-Sztul R, Phaeton R, Starr MD, Whitaker R, *et al*: Reciprocal SOX2 regulation by SMAD1-SMAD3 is critical for anoikis resistance and metastasis in cancer. Cell Rep 40: 111066, 2022.
44. Batlle E and Clevers H: Cancer stem cells revisited. Nat Med 23: 1124-1134, 2017.
45. Guha D, Saha T, Bose S, Chakraborty S, Dhar S, Khan P, Adhikary A, Das T and Sa G: Integrin-EGFR interaction regulates anoikis resistance in colon cancer cells. Apoptosis 24: 958-971, 2019.
46. Chen Z, Wang S, Li HL, Luo H, Wu X, Lu J, Wang HW, Chen Y, Chen D, Wu WT, *et al*: FOSL1 promotes proneural-to-mesenchymal transition of glioblastoma stem cells via UBC9/CYLD/NF-κB axis. Mol Ther 30: 2568-2583, 2022.
47. Li R, Che W, Liang N, Deng S, Song Z and Yang L: Silent FOSL1 enhances the radiosensitivity of glioma stem cells by down-regulating miR-27a-5p. Neurochem Res 46: 3222-3246, 2021.
48. Talukdar S, Pradhan AK, Bhoopathi P, Shen XN, August LA, Windle JJ, Sarkar D, Furnari FB, Cavenee WK, Das SK, *et al*: MDA-9/Syntenin regulates protective autophagy in anoikis-resistant glioma stem cells. Proc Natl Acad Sci USA 115: 5768-5773, 2018.
49. Kim SY, Hong SH, Basse PH, Wu C, Bartlett DL, Kwon YT and Lee YJ: Cancer stem cells protect non-stem cells from Anoikis: Bystander effects. J Cell Biochem 117: 2289-2301, 2016.
50. Xiong G, Ouyang S, Xie N, Xie J, Wang W, Yi C, Zhang M, Xu X, Chen D and Wang C: FOSL1 promotes tumor growth and invasion in ameloblastoma. Front Oncol 12: 900108, 2022.
51. Basu-Roy U, Seo E, Ramanathapuram L, Rapp TB, Perry JA, Orkin SH, Mansukhani A and Basilico C: Sox2 maintains self renewal of tumor-initiating cells in osteosarcomas. Oncogene 31: 2270-2282, 2012.
52. Ren C, Ren T, Yang K, Wang S, Bao X, Zhang F and Guo W: Inhibition of SOX2 induces cell apoptosis and G1/S arrest in Ewing's sarcoma through the PI3K/Akt pathway. J Exp Clin Cancer Res 35: 44, 2016.